The Thesis Committee for Alyse Colleen Briody
Certifies that this is the approved version of the following thesis:

Flow, nutrient, and stable isotope dynamics of groundwater in the parafluvial/hyporheic zone of a regulated river during a small pulse

APPROVED BY
SUPERVISING COMMITTEE:

Supervisor:

M. Bayani Cardenas

Kevan B. Moffett

Brad D. Wolaver

Flow, nutrient, and stable isotope dynamics of groundwater in the parafluvial/hyporheic zone of a regulated river during a small pulse

by

Alyse Colleen Briody, B.A.

Thesis

Presented to the Faculty of the Graduate School of

The University of Texas at Austin

in Partial Fulfillment

of the Requirements

for the Degree of

Master of Science in Geological Sciences

The University of Texas at Austin

August 2014

Acknowledgements

Bayani Cardenas — A big thank you for your guidance and encouragement during the past two years.

Kevan Moffett and Brad Wolaver — The input you provided was tremendously helpful and significantly improved this work.

My research Group: Lizhi Zheng, Lichun Wang, Peter Zamora, Kevin Befus, Raquel Flinker, Matt Kaufman, Eric Guiltinan, Aimee Ford, Mike Kanarek, Wen Deng — Thank you all for your academic and moral support and hard work in the Texas summer heat.

Others: Kim Myers, Jay Santillan, Jeff Senison, Wendy Robertson, Jasmine Mason, Mike O'Connor, Colin McNeece, Rosemary Hatch, Peter Carlson, Jenna Kromann, Brandon Okafor, Christina Barrera, and Patricia Bobeck — Each of you contributed to this work in some way and I greatly appreciate your efforts.

Kevin Anderson and Elisabeth Welsh- Thank you for sharing your abundant knowledge of the Hornsby Bend area and for allowing us to use the great AYRW facilities.

Laboratories: Philip Bennett and his HPLC and Carbon laboratories, Nate Miller and the Jackson School of Geosciences ICP-MS Laboratory, and Pin Shuai and Texas A&M University's Stable Isotope Geosciences Facility — Thank you for making this sample analysis possible.

Abstract

Flow, nutrient, and stable isotope dynamics of groundwater in the parafluvial/hyporheic zone of a regulated river during a small pulse

Alyse Colleen Briody, M.S. Geo.Sci

The University of Texas at Austin, 2014

Supervisor: M. Bayani Cardenas

Periodic releases from an upstream dam cause rapid stage fluctuations in the Colorado River near Austin, Texas. These daily pulses modulate fluid exchange and residence times in the hyporheic region, where biogeochemical reactions are pronounced. We installed two transects of wells perpendicular to the river to examine in detail the reactions occurring in this zone of surface-water and groundwater exchange. One well transect recorded physical water level fluctuations and allowed us to map hydraulic head gradients and fluid movement. The second transect allowed for water sample collection at three discrete depths. Samples were collected from 12 wells every 2 hours for a 24-hour period and were analyzed for nutrients, carbon, major ions, and stable isotopes. The results provide a detailed picture of biogeochemical processes in the bank environment during low flow/drought conditions in a regulated river. Findings indicate that a pulse that causes a change in river stage of approximately 16-centimeters does not cause

significant mixing in the bank. Under these conditions, the two systems act independently and exhibit only slight mixing at the interface.

Table of Contents

List of Tables

List of Figures

Chapter 1: Introduction and Background

1.1: HYPORHEIC EXCHANGE IN A REGULATED RIVER

Banks and riparian zones are often locations of hyporheic exchange wherein two flowpaths, each with a unique chemistry, interact. They have been described as locations of both "hot spots" and "hot moments", in terms biogeochemical processes and reaction rates (McClain et al., 2003).

Biogeochemical reactions are thought to occur at elevated rates within the hyporheic zone where microbes and solutes are able to interact within a porous substrate (Briggs et al., 2013; McClain et al., 2003). One such reaction is denitrification, the bacterially-mediated reduction and conversion of nitrate to nitrogen gas. The required factors for denitrification include a labile or accessible organic carbon source, a nitrate source, and suboxic redox conditions (Zarnetske et al., 2011). If organic carbon is available as an energy source and oxygen is depleted, nitrate will be the most energetically favorable terminal electron acceptor for denitrifying bacteria and denitrification will proceed (see equations below) (Briggs et al., 2013):

Nitrate Reduction: $NO_3^- + 2e^- + 2H^+ \rightarrow NO_2^- + H_2O$ (1)

Denitrification: $NO_3^- \rightarrow NO_2^- \rightarrow NO \rightarrow N_2O \rightarrow N_2$ (g) (2)

As a redox reaction: $2\ NO_3^- + 10\ e^- + 12\ H^+ \rightarrow N_2 + 6\ H_2O$ (3)

All fundamental ingredients for denitrification are potentially present within river banks.

Partly because of denitrification, the hyporheic zone has been described as a river's liver, with the ability to remove 37–76% of nitrogen input (Fischer et al., 2005). A study by Sjodin et al. (1997) showed that a large river removed half of the nitrogen input over the course of a year, presumably through denitrification (Sjodin et al., 1997). Other studies have shown that a significant portion of denitrification (14–97%) can be attributed to the hyporheic zone (Zarnetske et al., 2011). While the hyporheic zone is the suspected driver of this removal, limited direct field evidence has been reported (Harvey et al., 2013).

The saturated bank sediment can offer an organic carbon source and a low oxygen environment that are not present within the water column. Thus, they can be points of "streamside denitrification" (McClain et al., 2003). A study of decaying salmon-derived nitrogen examined nitrogen removal in the riparian hyporheic zone of an Alaskan river. The highest removal rate occurred during the first hour of nitrogen entering the bank. This was due to a combination of plant/microbial uptake and denitrification (Pinay et al., 2009).

A “hotspot” is an area where a nitrate supply converges with “missing reactants” (i.e. organic carbon rich reducing conditions); thus the entire bank is not necessarily a “hotspot.” The nitrate and “missing reactants” may be available intermittently, or during "hot moments" (McClain et al., 2003). In terms of water quality management, it is important to understand and be able to predict where and when these hot spots will occur.

The parafluvial zone, or the area of the channel that is dry during low-flow conditions, has also exhibited nutrient removal properties. Unlike a floodplain, the parafluvial zone is located within the bounds of the banks; it is the section of the channel that currently lacks surface water. It can shift in size and shape depending on changing river stage or flood events and has the potential to act as a source or a sink of nitrate. In a 1994 study, dye injected into the surface stream was collected in adjacent parafluvial gravel bars, verifying hydrologic linkage (Holmes et al., 1994). A decline of measured dissolved oxygen was observed along flowpaths in the parafluvial zone, but it rarely dropped below 5 mg/L. Dissolved oxygen levels in this range facilitate aerobic processes and nitrification, rather than denitrification. In this same study, water from the parafluvial region eventually returned to the nitrogen-limited stream environment via upwelling zones, thus acting as a nitrate source. However, under a different flow regime, a parafluvial zone could act as a nitrate sink (Holmes et al., 1994).

Chemical patterns in a hyporheic zone cannot be understood without considering the flow field and morphodynamics that govern it (Boano et al., 2010). Meandering

rivers, for example, promote hyporheic exchange in the intrameander region (Boano et al., 2010). In these settings, river sinuosity is the most influential characteristic in determining the produced hyporheic flow field, residence times, and biogeochemical zonation (Jones and Mulholland, 2000). In other systems, river regulation rather than sinuosity, is the dominant agent promoting this exchange (Sawyer et al., 2009).

For large rivers, damming or river regulation is the norm, with over 60% of rivers already dammed worldwide (McAllister et al., 2001). The Longhorn Dam, built in 1960, is one of seven dams spanning the Colorado River, which flows southeast across Texas and empties into the Gulf of Mexico. These dams were built to provide hydroelectricity, flood control, and storage for municipal, commercial, and agricultural customers.

The Lower Colorado River (LCR), the focus of this study, undergoes various degrees of hydropeaking, or rapid changes in water level caused by water releases from upstream dams, such as the Longhorn Dam (Figure 6). This hydropeaking behavior drives fluid flux in the hyporheic zone, the region where surface-water/groundwater exchange occurs and where chemical reactions and microbial activities are accentuated (Olde Venterink et al., 2003) (Figure 1). Thus, the chemistry of the LCR may be significantly affected by water level fluctuations and the enhanced hyporheic exchange they promote.

Although the LCR is typically considered to be a gaining river, increases in river stage have the potential to reverse hydraulic gradients and introduce periods of losing behavior during which surface water is driven into the streambed and adjacent banks (Larkin and Sharp, 1992; Sawyer et al., 2009). In these instances, the bank becomes a locus of hyporheic exchange. The degree of hyporheic flux is directly related to the magnitude of the stage fluctuations, with maximum stage heights causing the highest degree of hyporheic exchange in the bank environment (Gerecht et al., 2011).

In a study area in Virgina, Gu et al. modeled storm events in a creek and their effects on streambed sediments. These storm events, which can serve as an analog for dam releases, decreased groundwater input into the stream and increased surface water

residence time in the hyporheic zone. According to their model, shifting hydraulic gradients caused by the storm event provided increased opportunity for both denitrification and overall nitrate reduction to occur (Gu et al., 2008). The periodic man-made "storm events" in the LCR provide an ideal setting to further examine these processes.

The Clean Water Act Section 303(d) requires states to identify "impaired" water bodies and establish total maximum daily loads (TMDLs) of specific contaminants that are considered harmful to ecosystem health (EPA, 2012). Nutrient loading and excessive nitrate concentrations are common contributing factors to this "impairment", as they contribute to vegetation blooms and decreased dissolved oxygen concentration in the water column.

The stage fluctuations associated with river regulation increase the extent of the hyporheic zone and thus have the potential to affect the quality of surface water supplies (Gerecht et al., 2011). Increased awareness of these processes may have implications for the management of regulated and/or impaired rivers.

1.2: STUDY OBJECTIVES

The goal of the collection and analysis of these data is to contribute to the understanding of this complex environment.

Since the biogeochemistry of parafluvial and hyporheic zones of regulated rivers is understudied, we address the following open questions for the regulated LCR:

1. What are the processes controlling the chemical and isotopic patterns of hyporheic waters?
2. Does the bank provide the conditions necessary for denitrification to occur?
3. How much mixing (groundwater/surface-water) occurs in the bank?
4. Can we observe evidence of nitrate removal over the course of a pulse?

Our study uses direct field observations and chemical sampling to investigate groundwater/surface-water interactions and nutrient cycling at the Hornsby Bend site

along the LCR (Figures 2 and 7). We installed two transects of wells in the bank of the LCR. The first transect of wells was used to monitor water level fluctuations. The second transect was used to collect water samples at varying depths and analyze their chemical composition. By examining chemical data collected from within-bank sampling wells over a 24-hour period in August 2013 and interpreting the data along with stage and water table fluctuations, we obtained a detailed picture of the biogeochemical conditions present within the bank of this managed river, and thus were able to address the questions above.

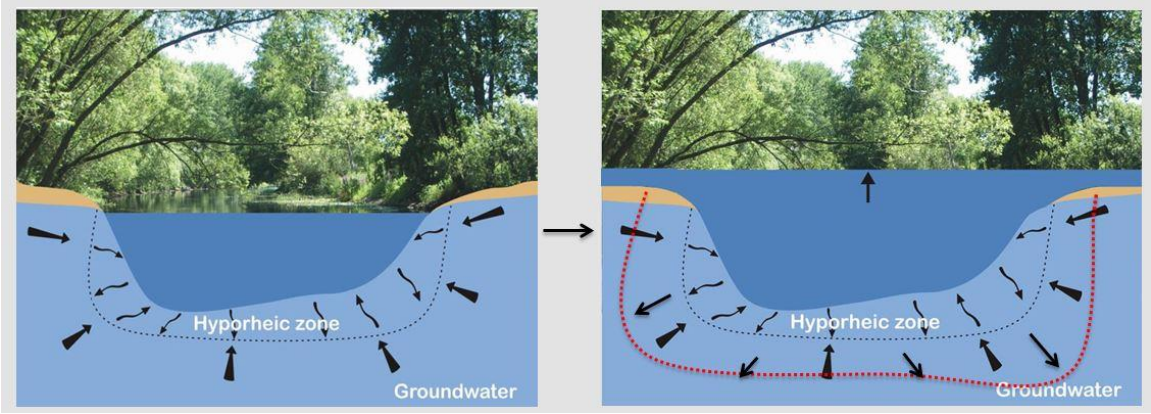

Figure 1: An increase in stage height increases hydraulic head in the river and forces surface water into the bank, enlarging the extent of the hyporheic zone (Image adapted from Leibniz-Institute of Freshwater Ecology and Inland Fisheries).

1.3: BACKGROUND ON THE STUDY SITE AND RELATED PREVIOUS STUDIES

The catchment area of the LCR is composed primarily of agricultural, urban, and residential land. It receives fertilizer-rich runoff and treated wastewater effluent and has historically contained elevated concentrations of nitrate (Colorado River Corridor Plan, 2012). A common pollutant in U.S. waterways, nitrate contributes to ecological and water quality issues at its eventual outlet, the Gulf of Mexico (Mitsch et al., 1999). By studying the dynamic water fluctuations associated with the Longhorn Dam, we can make inferences about the hydrologic and biogeochemical characteristics of regulated rivers in general.

Hornsby Bend is located 23 km downstream of downtown Austin, Texas, and the Longhorn Dam, which forms the eastern boundary of Ladybird Lake (Gerecht et al., 2011) (Figure 2). Before being designated an environmental research area, Hornsby Bend served as a quarry and grazing area, and some of the historic channels in this area have been dredged for gravel production.

The Walnut Creek Wastewater Treatment Plant is located approximately 3.2 miles north of Hornsby Bend (Figure 2). This treatment plant processes the majority of Austin's waste and discharges ~113 million gallons of treated effluent into the Lower Colorado River each day (Basin Highlights Report, 2014). While there is no regulatory limit on the nitrate concentration of the effluent, typical concentrations fall between 88 and 111 mg/L nitrate-NO_3^- (Raj Bhattarai, personal communication, August 12, 2014). When the LCR is operating under low-flow conditions, a higher percentage of total discharge is derived from treated wastewater. This can lead to an excess of nutrients and an overall increase in aquatic algae and vegetation (Basin Highlights Report, 2014).

The Colorado River Watch Network (CRWN) takes periodic water quality measurements at various locations along the LCR. The Montopolis Bridge monitoring station is located slightly upstream of the Walnut Creek Wastewater Treatment Plant while the Hornsby Bend monitoring station is located downstream. Nitrate data collected between 2011 and 2014 display significantly higher concentrations at Hornsby Bend than

Montopolis Bridge (Figure 3) (CRWN, 2014). This suggests an input of nitrate between the two sites, likely derived from the Walnut Creek Wastewater Treatment Plant.

Geologically, the study site is a combination of alluvium and terrace deposits composed of gravel, sand, silt, and clay. Sediments are primarily derived from Cretaceous and pre-Cretaceous limestone and chert, with minor contributions from older igneous and metamorphic rocks (Rodda et al., 1969). These unconsolidated deposits generally exhibit a fining-upwards sequence with gravel at the base. The terrace deposits are approximately 30 feet thick whereas the alluvium has a maximum thickness of 20 feet (Garner and Young, 1976).

While various sedimentologic units are present, they are interconnected and sediment variability allows for pathways of preferential flow (Gerecht et al., 2011). Some higher permeability pathways were mapped in 2011 using electrical resistivity (ER) imaging (Cardenas and Markowski, 2011). Based on previous measurements, the estimated hydraulic conductivity in the bank region is 2.25 meters/day with a porosity of 0.25 (Sawyer et al., 2009).

This area of the LCR is a gaining or baseflow-dominated system, where regional hydraulic gradients cause groundwater to flow toward the river (Larkin and Sharp, 1992). This behavior can be observed visually after driving a piezometer into the streambed and comparing the hydraulic head in the piezometer to the hydraulic head in the river (Figure 4). In March 2013, the head in the piezometer was measured to be 1.75 centimeters above the river stage. Using Darcy's law and a streambed hydraulic conductivity of 0.01 cm/s (8.64 m/d, estimated from a mix of sand and silt), this corresponds to a vertical flux of 3.78 cm/day of groundwater into the river.

In 2011, Cardenas and Markowski used electrical resistivity (ER) imaging to map and delineate groundwater/surface-water mixing zones in this same LCR area. The recorded resistivity values, which are related to chemical composition and sediment texture, could be used to distinguish between the more conductive groundwater end member and the more resistive surface water end member. While their study did not

focus on the bank, the authors delineated a zone of groundwater/surface-water mixing that extends several meters below the channel (Cardenas and Markowski, 2011).

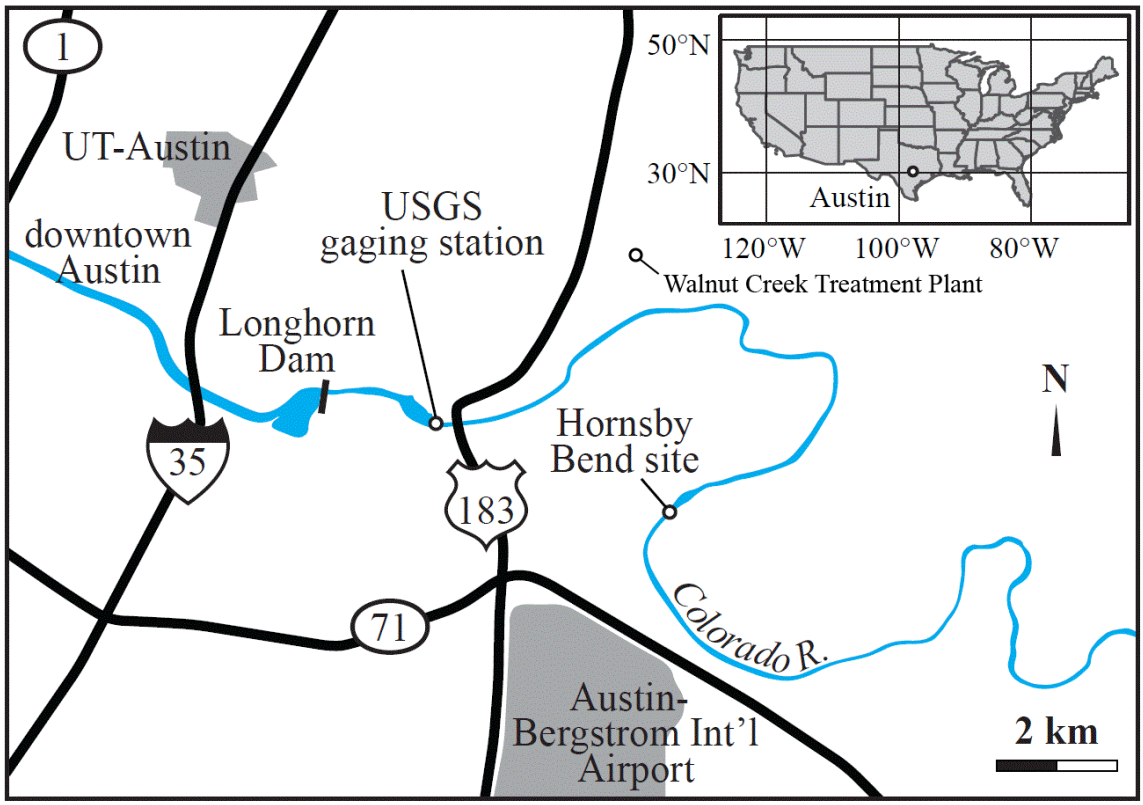

Figure 2: The location of the Hornsby Bend site in relation to downtown Austin, the Longhorn Dam, and the Walnut Creek Wastewater Treatment Plant (Sawyer et al., 2009).

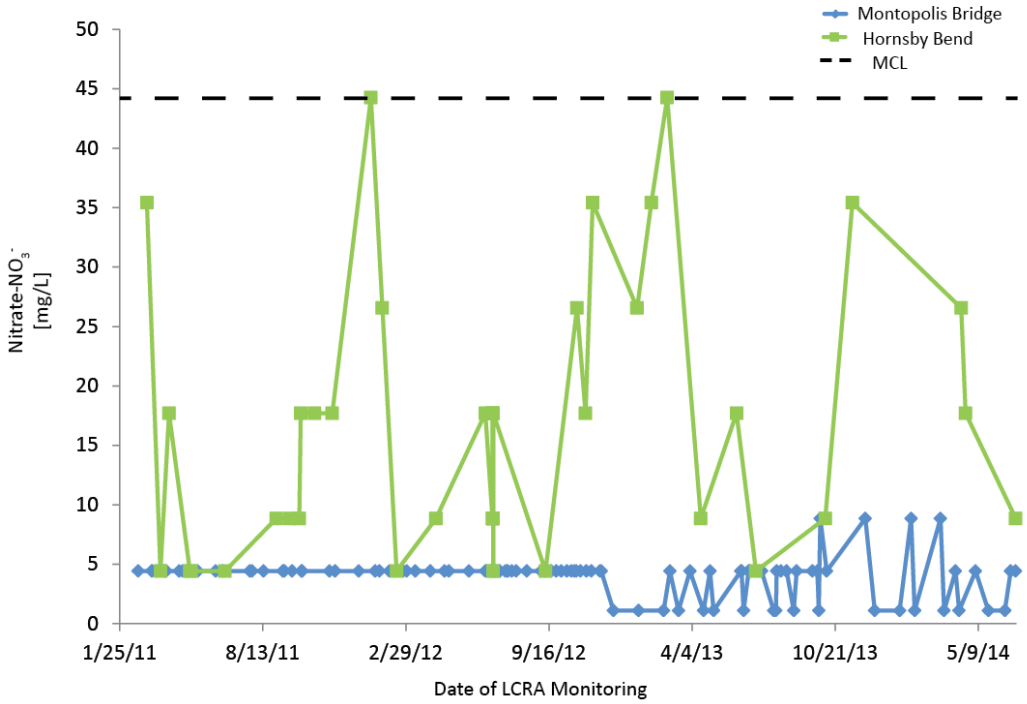

Figure 3: Concentrations of nitrate-NO_3^- [mg/L] measured at the Montopolis Bridge and Hornsby Bend monitoring stations (CRWN, 2014). The Walnut Creek Wastewater Treatment Plant is located between the two stations. The common maximum contaminant load (MCL) of 44 mg/L nitrate-NO_3^- is displayed with a dashed line.

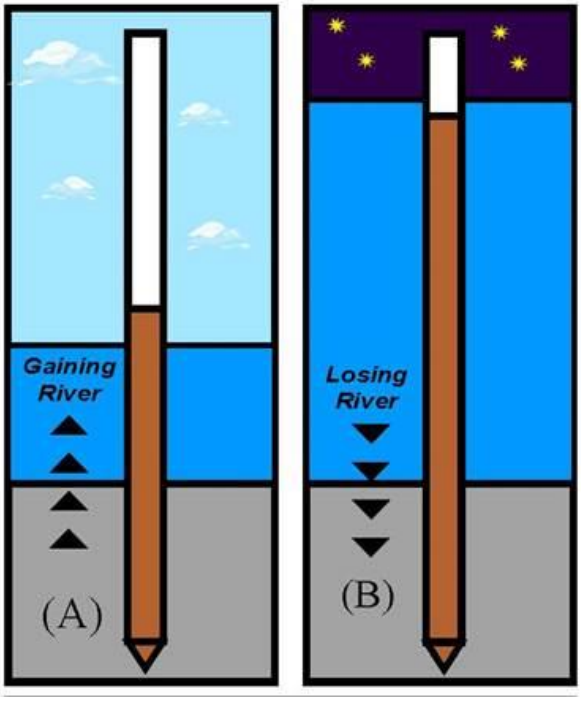

Figure 4: A gaining and losing river, defined by comparing the hydraulic head in the subsurface to the hydraulic head in the channel.

1.4: RIVER REGULATION REGIME

U.S. Geological Survey gauging station number 08158000 is located between the Longhorn Dam and Hornsby Bend, approximately two kilometers downstream of the dam and 11 kilometers upstream of the site. Daily oscillations in stage recorded by this gauge range from a few centimeters to more than a meter depending on the season and regional hydrologic conditions (Gerecht et al., 2011). The August 16-17, 2013 release during the 24-hour study period caused a relatively small river stage fluctuation of 16 centimeters at both the USGS gauge and the study site. This change in river stage caused water fluctuations (and corresponding fluxes) that extended into the bank (Figure 5).

The August 2013 water level shifts observed during this project were smaller than those that occur in a typical year (such as 2010) (Figures 5 and 6). The observed

conditions were not as dynamic as historically recorded in this system; they represented the muted river regulation associated with drought conditions. We chose to examine in detail the conditions at hand to understand riverbank and hyporheic function within this low-flow context.

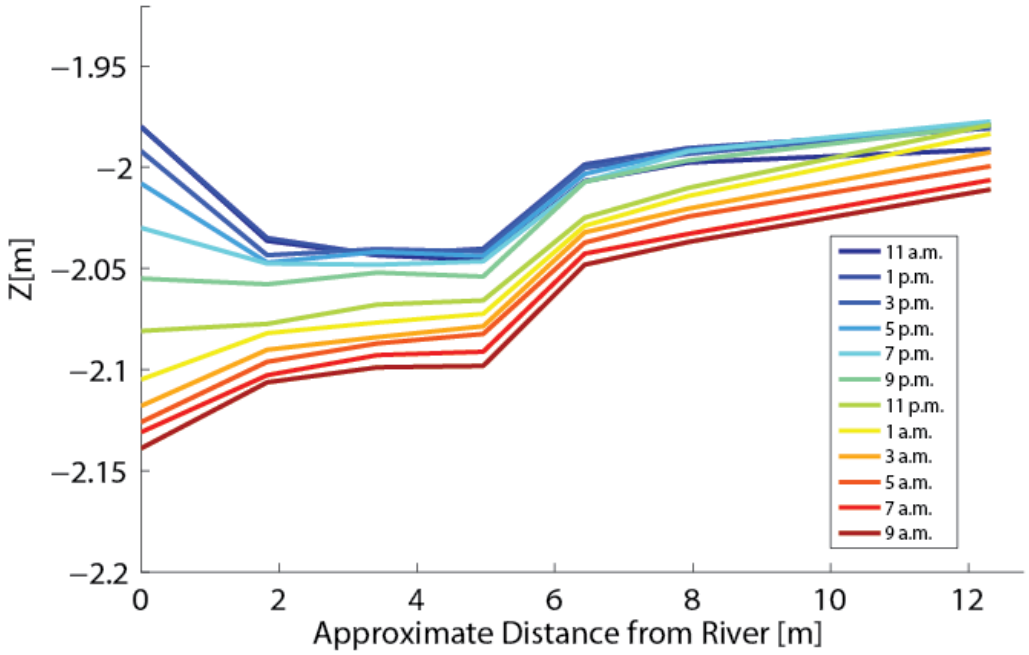

Figure 5: Water table elevations during a 24-hour sampling period, August 16-17, 2013.

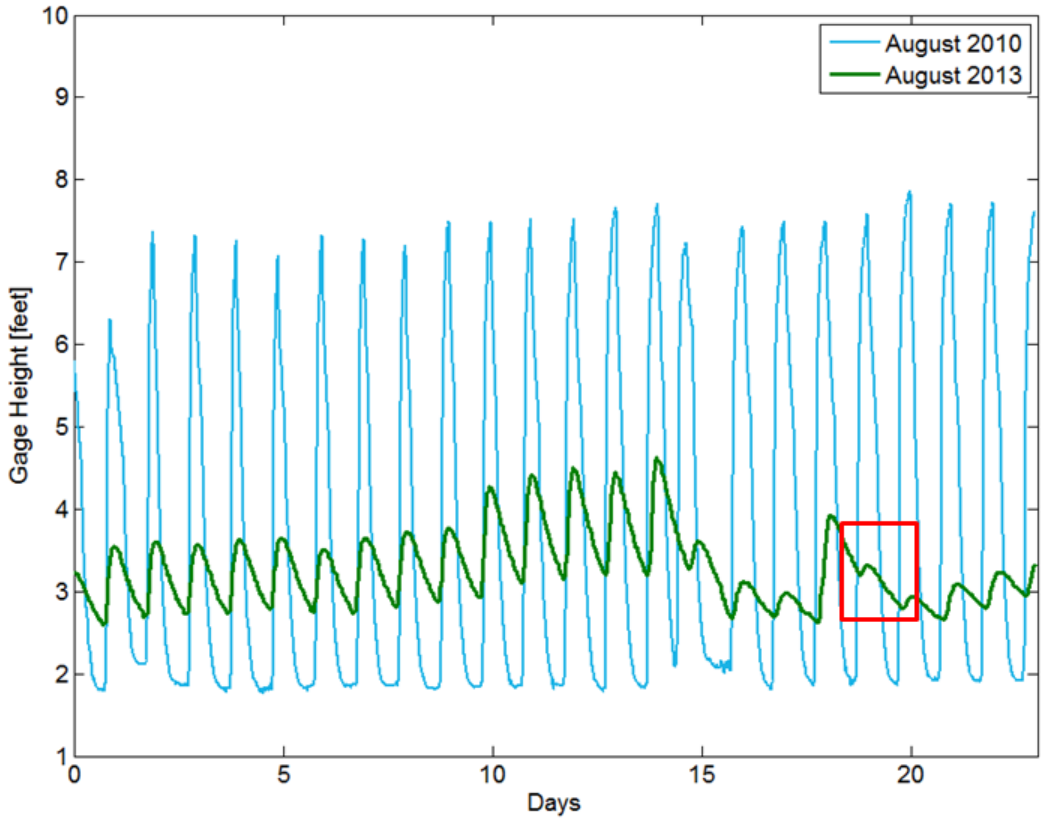

Figure 6: Comparison of periodic stage fluctuations in August 2010 and August 2013. Behavior observed in 2013 represents drought/low-flow conditions in a regulated river.

Chapter 2: Methods

2.1: Establishment of Study Transect

Before measurements or samples could be collected, the study site had to be set up. Preparation included the design and installation of seven monitoring wells, one stilling well, and twelve sampling wells.

Seven monitoring wells (piezometers) were installed via direct-push (Geoprobe) drilling. The wells were positioned in a transect perpendicular to stream flow, at increasing distances from the river. Piezometers were made of PVC and measured 3.175 centimeters (1.25 inches) in diameter. Monitoring wells were spaced approximately 1.5 meters apart, with the most landward monitoring well located 12.3 meters from the river. Screened intervals and locations are shown in Table 1.

Following monitoring well installation, twelve chemical sampling wells were installed manually using a hand auger. These piezometers were constructed of 3.175-centimeter diameter PVC pipe, with a 20 cm screened interval at the bottom. They were installed at three discrete depths (1.5, 2, and 2.5 meters below the ground surface or approximately 0.5, 1, and 1.5 meters below the water table). These chemistry sampling wells were arranged in a 3 × 4 grid to provide a shallow, medium, and deep transect of four wells each (see Figure 7 for layout and relative distances).

A stilling well was installed approximately 25 meters upstream of the monitoring wells. Two 3.048 meter (10-foot) pieces of 10.16 centimeter (4-inch) diameter PVC were connected at a right angle with an elbow joint. The portion of the pipe in the river was perforated to allow for water to enter and exit freely. The L-shaped stilling well was then buried into the bank to allow for monitoring of changes in river stage. Ground surface and top-of-casing piezometer positions and elevations were surveyed using a total station (Table 1) accurate to <1 mm (S3 Total Station, Trimble Navigation, Ltd., Sunnyvale, CA).

Well	E (X) [m]	N (Y) [m]	Z (Ground Surface) [m]	Z (Top of Casing) [m]	Total Depth from Ground Surface	Screened Interval [m]
MW7	0.84	-2.78	0.048	0.958	3.658 m (12 feet)	-3.658 to -1.219 (-12 to -4 ft.)
MW6	0	0	-0.228	0.66	3.658 m (12 feet)	-3.658 to -1.219 (-12 to -4 ft.)
MW5	-1.40	4.35	-0.922	-0.039	3.048 m (10 feet)	-3.048 to -0.610 (-10 to -2 ft.)
MW4	-1.78	5.78	-0.926	0.057	3.048 m (10 feet)	-3.048 to -0.610 (-10 to -2 ft.)
MW3	-2.25	7.2	-1.015	0.009	3.048 m (10 feet)	-3.048 to -0.610 (-10 to -2 ft.)
MW2	-2.69	8.64	-1.116	-0.092	3.048 m (10 feet)	-3.048 to -0.610 (-10 to -2 ft.)
MW1	-3.17	10.15	-1.446	-0.431	2.134 m (7 feet)	-2.134 to -0.610 (-7 to -2 ft.)
Stilling Well	21.14	16.49	N/A	0.706	N/A	N/A

Table 1: Piezometer positions and elevations. Well MW-6 was established as local geographic origin (X0,Y0).

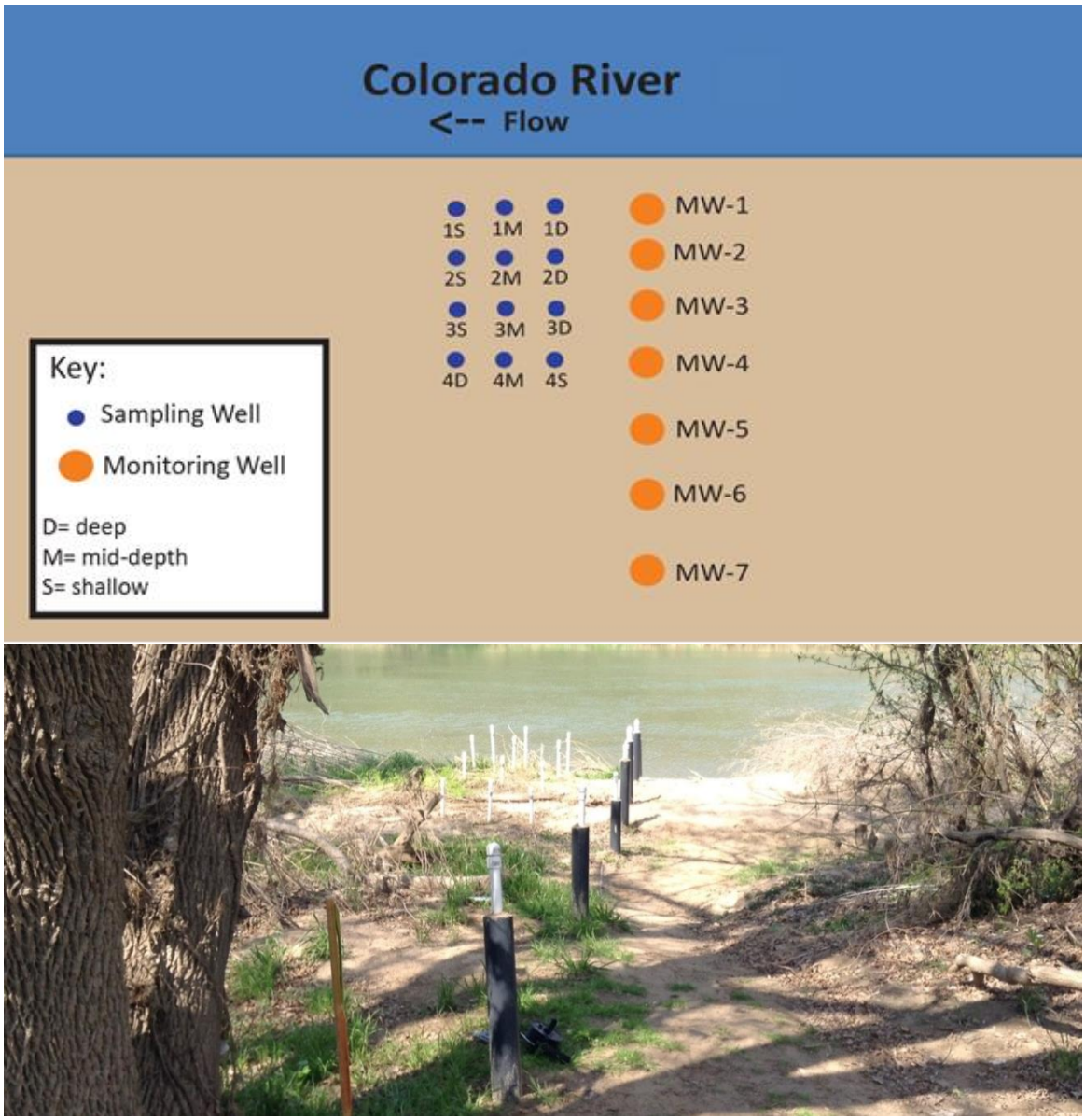

Figure 7: Plan and photographic views of the study site showing the relative locations of sampling and monitoring wells.

2.2: HYDRAULIC MONITORING AND FLUID FLUX ESTIMATION

Pressure transducers (AquaTroll 200, RuggedTroll 100, Rugged BaroTroll, In-Situ Inc., Ft. Collins, CO) were installed in six monitoring wells (MW1–MW5, MW-7) and the stilling well (to monitor changes in river stage). The transducers recorded water level every five minutes, thus providing information about shifting water levels and hydraulic gradients. Multiple water level tape measurements taken throughout the sampling campaign were used to convert transducer data to physical water table elevations, and for spot checking. Using the water table elevations, horizontal groundwater flow velocities (Darcy fluxes) were calculated using Darcy's law.

2.3: TWENTY-FOUR HOUR SAMPLING CAMPAIGN

Samples were collected during a 24-hour time period because hydropeaking water level fluctuations typically occur within this interval at this site. Samples were collected from each well and the river every two hours for 24 hours for a total of twelve sampling periods. Sampling began at 11 a.m. on August 16, 2013, and ended at 9 a.m. on August 17, 2013 (Figure 8). Five samples were collected from each well during each sampling time step including: 125 mL bottle of raw, unfiltered water, 30 mL acid-washed bottle for cation analysis (acidified), 30 mL bottle for anion analysis, 40 mL glass bottle for carbon analysis, and a 4 mL glass bottle for hydrogen and oxygen isotope analysis (Figure 9). Samples were filtered with a 0.22 μm syringe filter.

A sample set was also collected from the monitoring well furthest from the river (MW-7) as the background groundwater for this system. Given its location approximately 12.3 m from the river, we expect this groundwater to have minimal exposure to the river water. At 3.66 meters below the ground surface, it extends deeper than the bank wells (at 1.5–2.5 meters below ground surface). Due to the predominant regional hydraulic gradient in this area, we assume a consistent groundwater source across this range of depths (Larkin and Sharp, 1992).

Peristaltic pumps were used to collect water samples from all wells. After purging approximately three well volumes, sample bottles were rinsed and filled using a 60 mL syringe. Blanks and replicates were collected periodically throughout the 24-hour sampling period. After collection, samples were stored on ice in coolers until they could be transported to a laboratory refrigerator.

Figure 8: Sample collection from the 12 sampling wells.

Figure 9: Chemical sampling bottles. Left to right: Raw sample, carbon, cations, anions, and stable isotopes.

2.4: LABORATORY ANALYSES METHODS

2.4.1: Dissolved Inorganic and Organic Carbon, and alkalinity

Dissolved Inorganic Carbon (DIC) and Dissolved Organic Carbon (DOC) were measured using a Teledyne Tekmar Combustion Total Carbon Analyzer. Detection range for the analyzer is 4 ppb to 25000 ppm Carbon. The computer program TOC Talk/Apollo 9000 was used to analyze calibration curves and results.

DIC, the sum of inorganic carbon species in a solution, is comprised of carbon dioxide, carbonic acid, bicarbonate, and carbonate species:

$C_T = CO_2 + H_2CO_3 + HCO_3^- + CO_3^{2-}$ (4)

DIC (or C_T) is a function of the pH of the system as well as the rock/water interaction that occurs within the aquifer. Alkalinity refers to the acid neutralizing capacity of a water, also known as the sum of the titratable bases. We can convert from DIC concentration to alkalinity by calculating α_{HCO3}^-, the bicarbonate component (i.e. fraction) of the total DIC (Kalff, 2002). From α_{HCO3}^-, we can calculate alkalinity directly (assuming that alkalinity is derived solely from bicarbonate). Dissociation constants (K_1 and K_2) and the laboratory-measured pH value were used to calculate α_{HCO3}^- (equation 5). With this fraction, DIC concentration was converted to alkalinity (equation 6).

$$\alpha_{HCO_3^-} = \frac{1}{\frac{[H^+]}{K_1} + 1 + \frac{K_2}{[H^+]}} \qquad (5)$$

$$DIC \cong \frac{Alk}{\alpha_1} \approx Alk\left(\frac{[H^+]}{K_1} + 1\right) \qquad (6)$$

Dissolved organic carbon (DOC) is a measure of organic material dissolved in solution. In this study, "dissolved" refers to less than 0.22 μm because of the filter size used. For our purposes, DOC is used as a gauge for total organic carbon, the energy source available to denitrifying bacteria.

2.4.2: Stable isotopes of water

Hydrogen ($^{2}H/^{1}H$) and oxygen ($^{18}O/^{16}O$) isotopes provide information about the history of a water sample. During the fractionation process, the lighter isotope leaves the system and the heavier isotope remains behind, causing water to become enriched in the heavy isotope. As a result, variation $^{18}O/^{16}O$ and $^{2}H/^{1}H$ ratios can be used to determine the source, evaporation history, or mixing history of water (Kendall and McDonnell, 1998).

Oxygen and hydrogen isotopes were analyzed at Texas A&M University's Stable Isotope Geosciences Facility using a Picarro Cavity Ring-Down Spectrometer (Picarro WS-CRDS). Measurements were standardized using the Vienna Standard Mean Water (VSMOW) and data were reported using the following notation:

$$\delta\ ‰ = (R_{sample}/R_{standard} - 1) \times 1000 \qquad (7)$$

where R is the $^{18}O/^{16}O$ or $^{2}H/^{1}H$ ratio and δ is the deviation from the V-SMOW standard (in parts per thousand). Positive ratios (δ values) signify enrichment of the heavy isotopes while negative values signify depletion.

Stable isotope measurements are typically compared to the Global Meteoric Water Line (GMWL) and Local Meteoric Water Line (LMWL). The GMWL has a slope of ~8 (on a $\delta^{2}H$ vs. $\delta^{18}O$ plot), whereas arid regions that undergo more evaporation have LMWL slopes that range from 4 to 6. Comparison of samples to the GMWL and LMWL can provide insight about evaporative history (Kendall and McDonnell, 1998).

The LMWL for this analysis comes from Briggs, Texas, (Station ID: 08103900) located 50 miles north of Austin; this area has the same "humid subtropical" climate classification as Austin (Kottek et al., 2006). The equation for the LMWL is $\delta^{2}H = 4.93\ \delta^{18}O - 3.5$, which is indicative of an evaporative climate (Coplen and Kendall, 2000).

The amount of evaporation can be estimated using the Rayleigh fractionation equation. The Rayleigh fractionation equation is a function of the fraction of the reservoir remaining (f) and the fractionation of vapor relative to liquid (ε) (Aeschbach-hertig, 2012).

$\delta = (1+\delta_0)\, f^{\varepsilon} - 1$ (8)

where $\varepsilon = -9.29$ for $\delta^{18}O$ at 25 °C.

2.4.3: Major anions and cations

A High Precision Liquid Chromatograph (HPLC) was used to measure anion concentrations of the water samples. The apparatus consists of an autosampler, a pump, a chromatography column, an absorbance detector, and a conductivity detector. Prior to analysis, samples were filtered with IC-Na cartridges (Maxi-Clean IC-Na, Alltech, Grace, Columbia, MD). Filtration exchanges cations for sodium, preventing cations from damaging the chromatography column. Post analysis, we used PeakSimple chromatography software to integrate the area of absorbance and conductivity peaks and convert them to a concentration. Nitrate (as NO_3), nitrite, and chloride were measured.

Nitrate is a nutrient and contaminant commonly found in waterways. Excess amounts can result from agricultural/urban runoff or wastewater input into a stream. When in abundance, nitrate contributes to hypoxia and may be harmful to ecological health. Nitrite is of potential interest because it represents an intermediate phase in denitrification; by measuring nitrite we can observe the denitrification process as it occurs. Knowledge of chloride is useful because chloride is considered to be non-reactive/conservative; that is, its relative concentration does not change/transform as it moves through a watershed. Therefore, it can be a useful tool to explore flow paths and mixing within a system.

Cations were analyzed in the quadrupole inductively coupled plasma mass spectrometry (ICP-MS) Lab at the University of Texas at Austin. The ICP-MS has the ability to measure cations at low concentrations/detection limits. Before analysis, samples were diluted (10×) with 2% nitric acid.

Cation concentration is a function of the surrounding geologic media and the degree of rock-water interaction. Major cations can be used to characterize the general

chemistry of various waters/sampling locations. Here, we also analyze the major ion data by plotting Stiff diagrams using the software RockWare AqQA. Charge balance was calculated for a random subset of the samples (including at least one for each well). All samples fell below 5% charge balance error (Appendix Table A1).

2.4.4: Dissolved Oxygen

Dissolved oxygen (DO) was measured in the field with an Oakton DO Meter (OAKTON Instruments, Vernon Hills, IL). A peristaltic pump and a beaker were used to collect water from each sampling well and take "flow-through" measurements. Dissolved oxygen measurements are used to determine the redox conditions of sampling locations. Dissolved Oxygen measurements were taken after the 24-hour sampling event (on March 6, 2014). While water levels in the sampling wells were not identical on this day (as the river stage was approximately 0.7 meters lower), measured DO values provide an estimate of expected dissolved oxygen levels in the bank environment.

2.4.5: Characterization of variation over 24-hours

Standard deviation and percent relative standard deviation were used to determine the degree of variability at each sampling point through time.

Percent Relative Standard Deviation (%RSD) = $\left(s \div \mu\right) \times 100$ (9)

where s is the sample standard deviation and μ is the sample mean.

Chapter 3: Results, Discussion, and Conclusions

3.1: GROUNDWATER FLUXES

Water table elevations and well positions were used to calculate Darcy flux at each time step (Figure 10). A positive Darcy flux corresponds to water flowing into the bank while a negative Darcy flux corresponds to water flowing out of it. Based on the calculations of horizontal Darcy flux through time, surface water was flowing into the bank during the first three time periods. However, the gradients and fluxes quickly diminished away from the river, with minimal movement occurring in the region 1.8 to 3.4 meters from the river (between monitoring wells 1 and 2). Relatively high groundwater flow toward the river was observed 5.0 to 6.4 meters into the bank (between wells 3 and 4). This was likely due to the change in topographic slope that was present between those two well locations. Through time, the apparent flux past all wells became more negative, i.e. directed more strongly toward the river. This behavior agreed with the decreasing stage recorded in the river and captured the falling limb of the hydrograph.

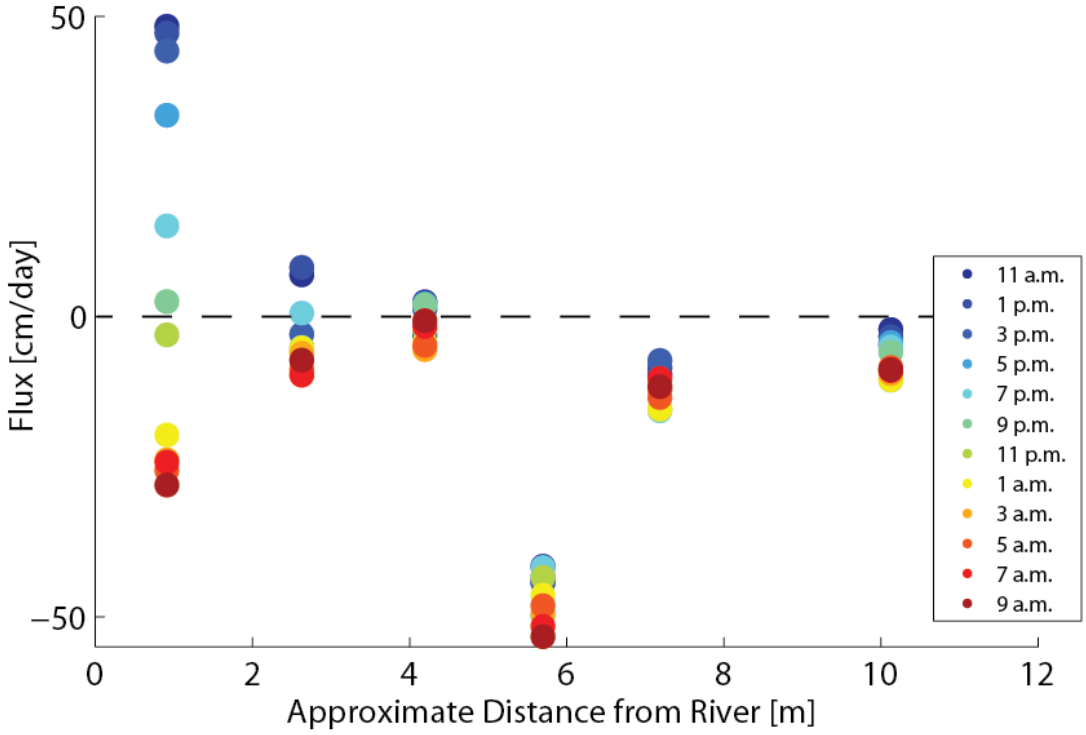

Figure 10: Horizontal Darcy flux during 24-hour sampling period [cm/day]. Water table measurements were taken from MW1–5 and MW-7.

3.2: CONDITIONS FOR DENITRIFICATION

Results of chemical analyses are presented as two-dimensional (2D) vertical sections (shown in Figure 11) with letters referring to shallow (S), mid-depth (M), and deep (D). Colors correspond to the color bar shown on the figure. The river is located to the left of wells 1S, 1M, and 1D.

First we discuss the presence of critical denitrification ingredients (sufficient nitrate, suboxic conditions, and carbon availability) at this site. During the 24-hour sampling period, nitrate values in the river ranged from 9–30 mg/L whereas nitrate in the bank ranged from 0–6 mg/L (Figures 12 and 13). No spatial pattern was observed in the bank as all values were relatively low and consistent (Appendix Table A8). The concentrations measured in the river are typical for agricultural streams and are considered to be high (Dubrovsky and Hamilton, 2010). Based on the consistently high concentrations measured, the river represents a potential source of nitrate in this system. Minimal quantities of nitrite were measured in sampling wells (all below the detection limit). Nitrite values in the river were also very low, ranging from 0 to .4 mg/L (Appendix Table A9).

DO in the bank ranged from 0.58 to 1.35 mg/L (Figure 14, Appendix Table A5). This is equivalent to 7–16.5% saturation and represents suboxic conditions (USGS DO table). Dissolved oxygen in the river was measured at 8–10 mg/L (LCRA 2013). The depleted oxygen levels in the bank create redox conditions supportive of denitrification.

DOC existed in fairly uniform concentrations in both the river and the adjacent bank. All values fell within a range of 4–8 mg/L except for the background groundwater (MW-7) which ranged from 3.4–10.8 mg/L (Figure 15). The river and Transect One (closest to the river) showed the highest variability in DOC and well 1S had consistently higher levels than the surrounding wells (Appendix Table A7). However, measured levels at all sites represent abundant organic carbon that can be used as a food source for denitrifying bacteria.

The three critical components of denitrification (i.e., a source of nitrate, abundant organic carbon, and a suboxic redox environment) appear to be present in this setting.

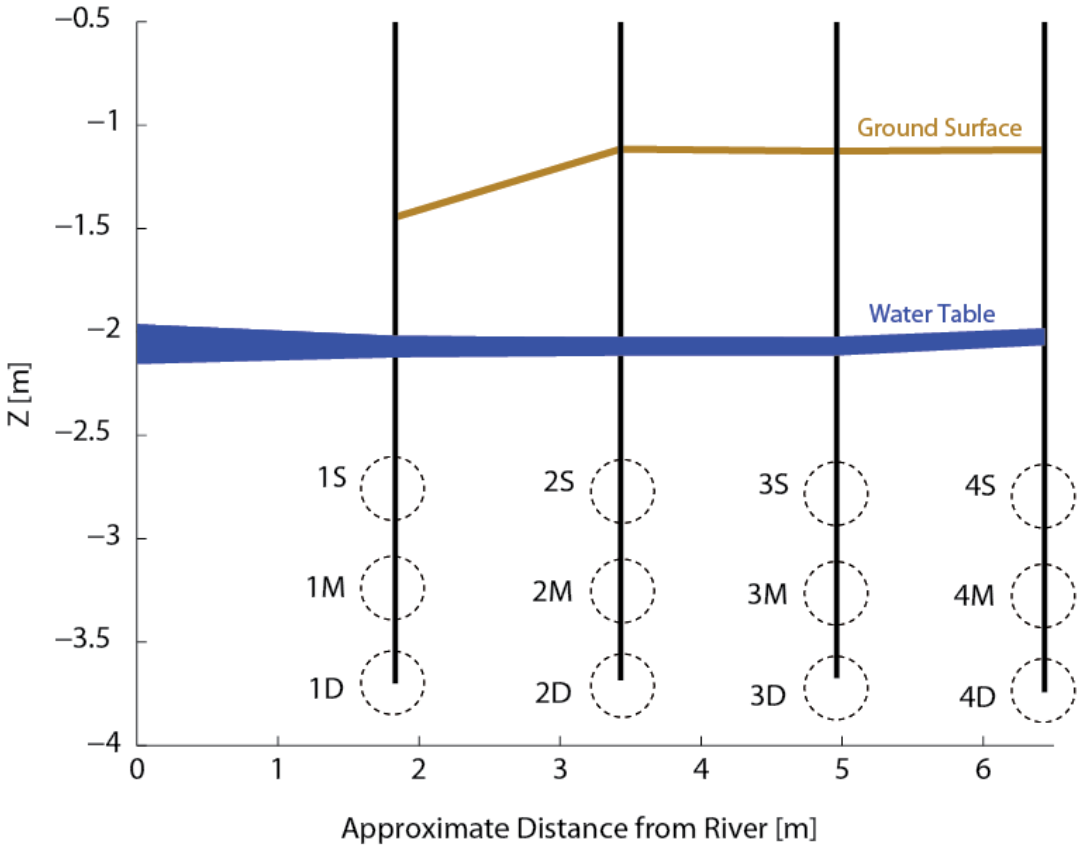

Figure 11: Two-dimensional (2D) vertical section showing relative locations of sampling wells. Letters refer to shallow (S), mid-depth (M), and deep (D) sampling piezometer screens.

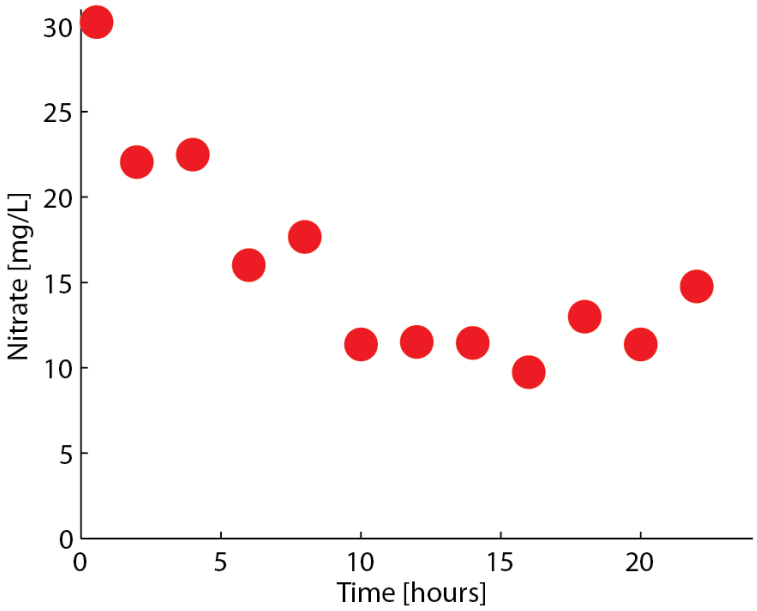

Figure 12: Concentrations of nitrate-NO_3^- [mg/L] in the river during the 24-hour sampling period. Elevated levels suggest the river as a potential source of nitrate. Time=0 corresponds to the beginning of the sampling period (i.e., 11 a.m. on August 16, 2013).

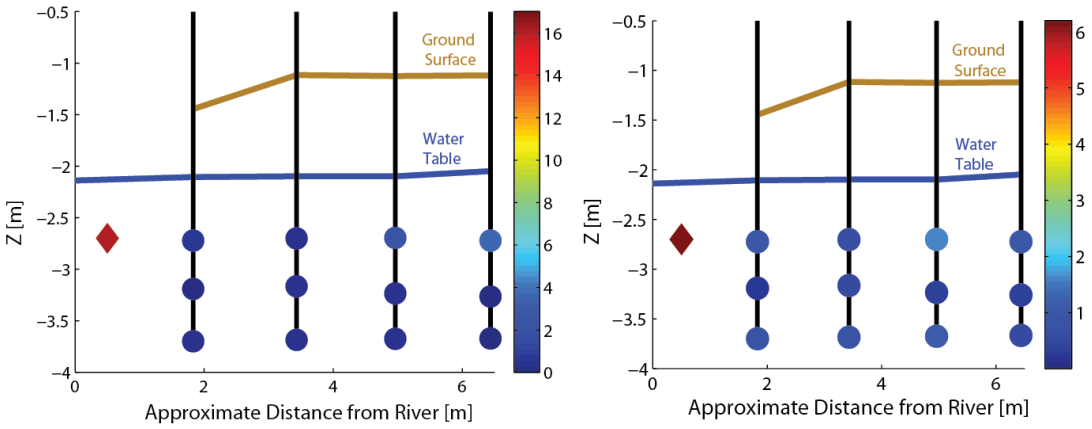

Figure 13: Two-dimensional (2D) vertical section of daily average nitrate-NO_3^- [mg/L] (left) and standard deviation of nitrate-NO_3^- [mg/L] during the 24-hour sampling period (right). Nitrate in MW-7 ranged from 0–5.4 mg/L.

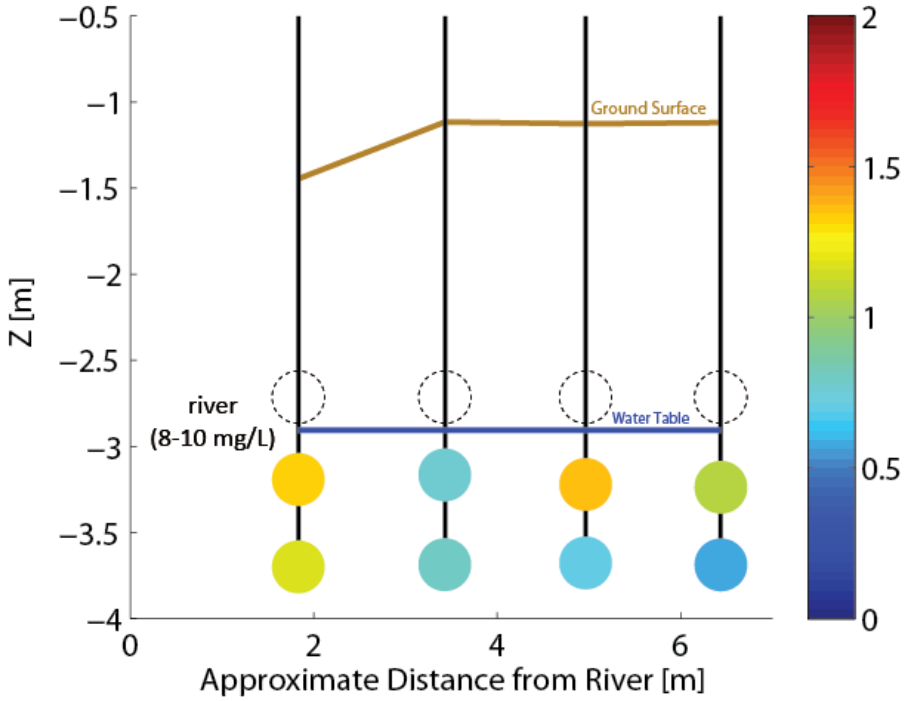

Figure 14: A dissolved oxygen [mg/L] vertical profile of the sampling wells indicating oxygen depletion in the bank. Empty circles refer to dry wells.

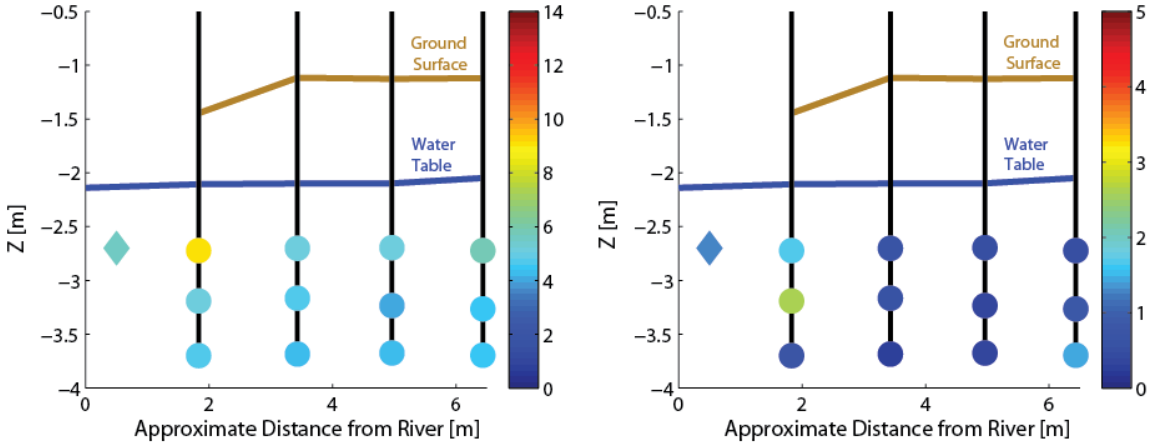

Figure 15: Two-dimensional (2D) vertical section of daily average dissolved organic carbon (DOC) [mg/L] (left) and standard deviation of DOC [mg/L] (right) during the 24-hour sampling period. DOC in MW-7 ranged from 3.4–10.8 mg/L. Elevated values are present in both the river and the bank environment.

3.3: RIVER-GROUNDWATER MIXING ANALYSIS

To evaluate mixing of groundwater and surface-water that may occur the bank, we took three approaches; we looked at DIC and chloride concentrations as indicators of mixing (due to the contrasting average concentrations in the river versus the bank), we developed a binary mixing model for $\delta^{18}O$ and chloride, and we identified spatial patterns in chemistry with Stiff Diagrams.

3.3.1: Dissolved Inorganic Carbon (DIC)

Throughout the sampling period, DIC concentrations in the river were much lower than those in the bank and background groundwater. River values ranged from 31–43 mg/L while bank values ranged from 98–120 mg/L (Figure 16, Appendix Table A6). The DIC concentration in the background groundwater (MW-7) was 112 mg/L. The increased levels in the bank are likely due to increased interaction with the surrounding geologic media. Surface water interacts less with rock and has less opportunity to dissolve inorganic carbon species. The distinct concentration (end-member) present in the surface water makes it easy to discern mixing behavior. An influx of surface water would be expected to drastically lower the DIC concentration in the bank.

By observing the total DIC change in a well during the 24-hour sampling period, it is possible to infer the amount of mixing that has occurred at that particular site. Relative change indicates the degree to which surface water has been introduced into the well.

Based on the calculated relative standard deviation [%], mixing was most pronounced in wells 1S and 2M (Figure 16, Appendix Table A6). Well 1S is located closest to the river channel and is expected to be readily influenced by its fluctuations. The high relative standard deviation in Well 2M suggests that it is hydraulically well-connected to Well 1S.

3.3.2: Chloride

Similar to the contrast that was observed in DIC (but on a less exaggerated scale), chloride concentrations in the river were much lower than those measured in the bank. Chloride in the river ranged from 43–76 mg/L while the bank maintained higher chloride values of 98–125 mg/L (Figure 17, Appendix Table A10). The background groundwater (MW-7) had a chloride range slightly lower than the bank at 92–110 mg/L. Chloride displayed an overall pattern similar to DIC, with 1S and 1M exhibiting a slightly higher %RSD than surrounding wells. However, chloride variability is higher overall and a clear pattern is not recognizable.

It is assumed that chloride is introduced to the system via rainfall and dry deposition, as chloride is not a significant component of the surrounding geology. However, the nearby sewage treatment settling ponds are another potential source of chloride. It is unknown whether or not settling pond effluent reaches this sampling area, but regional hydraulic gradients allow the possibility. This could account for higher chloride concentrations in the groundwater than in the river. An additional contributing factor is likely evapo-concentration in between precipitation events, which would cause chloride concentrations to steadily increase with time.

3.3.3: Binary mixing model and evaporative model

A binary mixing model was used to evaluate mixing in the bank environment. Chloride and $\delta^{18}O$ were chosen as parameters because they are expected to be relatively conservative within the watershed. If we plot the $\delta^{18}O$ and chloride concentrations of our surface-water and groundwater end-members, any "mixture" of the two would be expected to fall somewhere in between (on a binary mixing line) (Figure 18).

Results indicate that the bank samples had chloride concentrations similar to the groundwater end-member, yet they were enriched in $\delta^{18}O$. The surface water also showed enrichment in $\delta^{18}O$. Evaporation was the likely cause of this phenomenon, as it would increase $\delta^{18}O$ in both the river and the shallow subsurface. The Rayleigh fractionation

equation (8) was used to approximate the fraction of the original reservoir remaining (assuming that the original reservoir was groundwater). In other words, the equation estimated the amount of evaporation necessary to arrive at the values measured in the bank. Given this framework, the bank samples exhibited 4–6% evaporative loss (causing an enrichment of $\delta^{18}O$ and a deviation from the groundwater end-member).

This signature is logical given that bank samples were taken at a depth of 5–8 feet while the groundwater end-member was taken from a depth of 12 feet. Based on the $\delta^{18}O$-Cl^- mixing model, the bank water closely resembles the groundwater, except for a slight signature of evaporation.

Sample δ^2H and $\delta^{18}O$ values were also plotted in relationship to the Global Meteoric Water Line (GMWL) and Local Meteoric Water Line (LMWL) for Briggs, Texas to understand their isotopic composition in a regional context (Figure 19). The Hornsby Bend samples track very closely with the LMWL. The groundwater end-member has a distinct composition while surface water and bank samples overlap. This trajectory coincides with our evaporation hypothesis, with river and bank samples falling further along the LMWL in the evaporative direction.

3.3.4: Stiff diagrams

Stiff diagrams were used for visual comparison of general chemical patterns in all wells (Figure 20). Daily averages were used to plot a representative stiff diagram for each sampling location. The resulting diagrams showed that the chemical composition of bank samples closely resembled background groundwater. The river, however, maintained a distinct composition. This method for investigating qualitative mixing revealed no obvious locations of intermediate chemical composition. We can conclude that minimal mixing occurred during this sampling period.

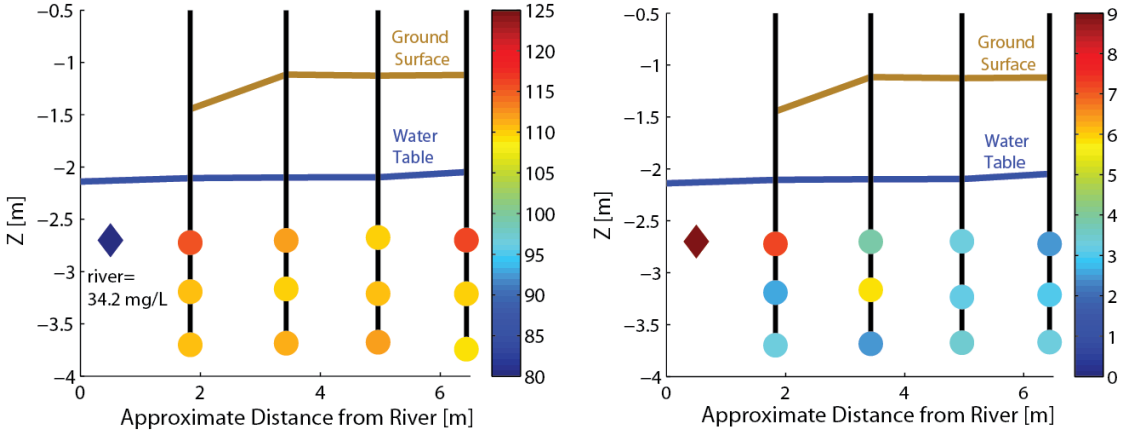

Figure 16: Two-dimensional (2D) vertical section of daily average dissolved inorganic carbon (DIC) [mg/L] (left) and relative standard deviation of dissolved inorganic carbon over 24 hours [%] (right). The concentration in MW-7 was 112 mg/L.

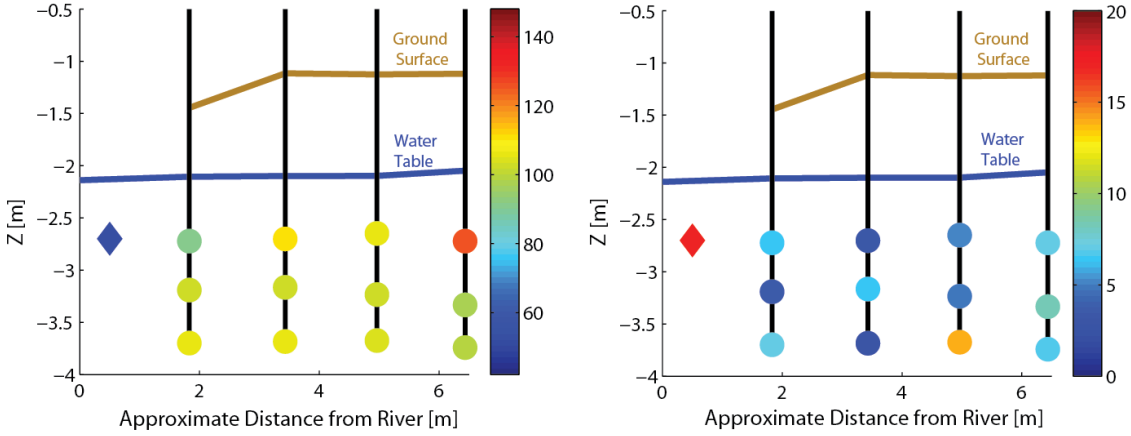

Figure 17: Two-dimensional (2D) vertical section of daily average chloride [mg/L] (left) and relative standard deviation of chloride during 24-hour sampling period [%] (right). The concentration in MW-7 ranged from 92–110 mg/L.

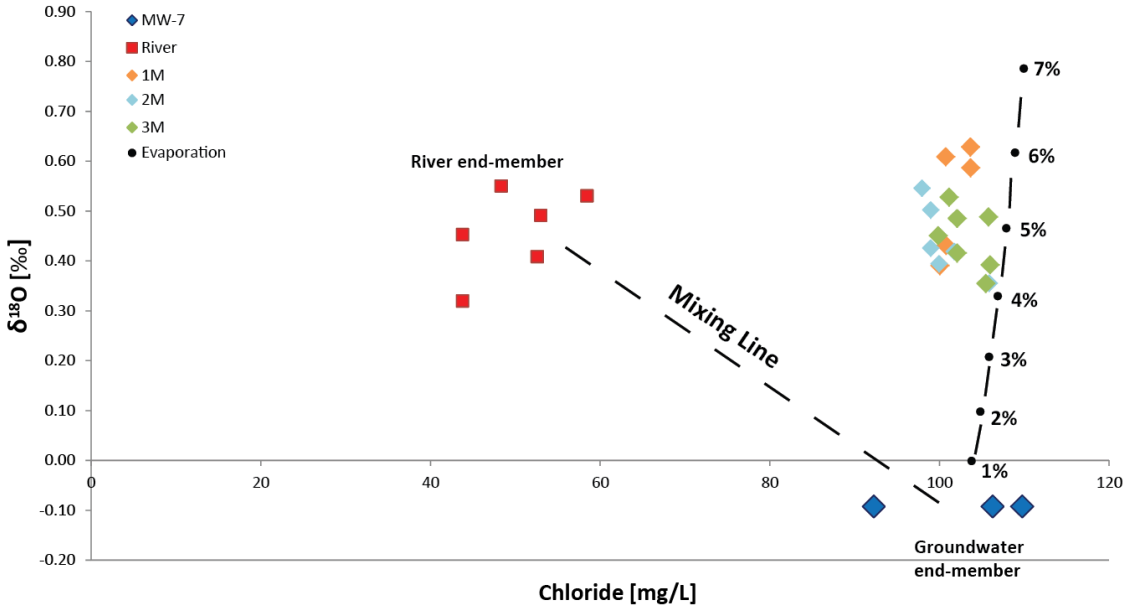

Figure 18: Binary mixing model based on the relationship between chloride and $\delta^{18}O$. Sampling wells fall on an evaporation deviation rather than on a simple mixing line between the surface water and groundwater end-members. Percentages indicate amount of evaporation necessary to reach a given concentration (i.e., 1% evaporation= 99% original reservoir remaining).

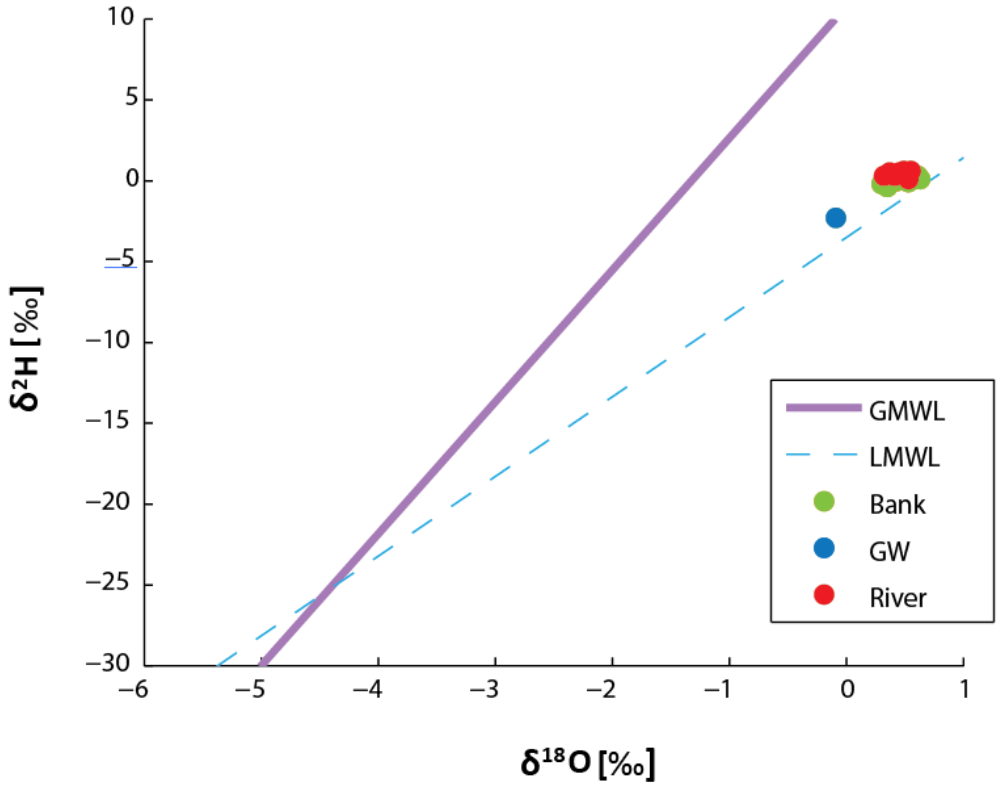

Figure 19: The relationship between hydrogen and oxygen isotope ratios in Hornsby Bend samples as compared to the Global Meteoric Water Line (GMWL) and Local Meteoric Water Line (LMWL) of Briggs, Texas (Coplen and Kendall, 2000).

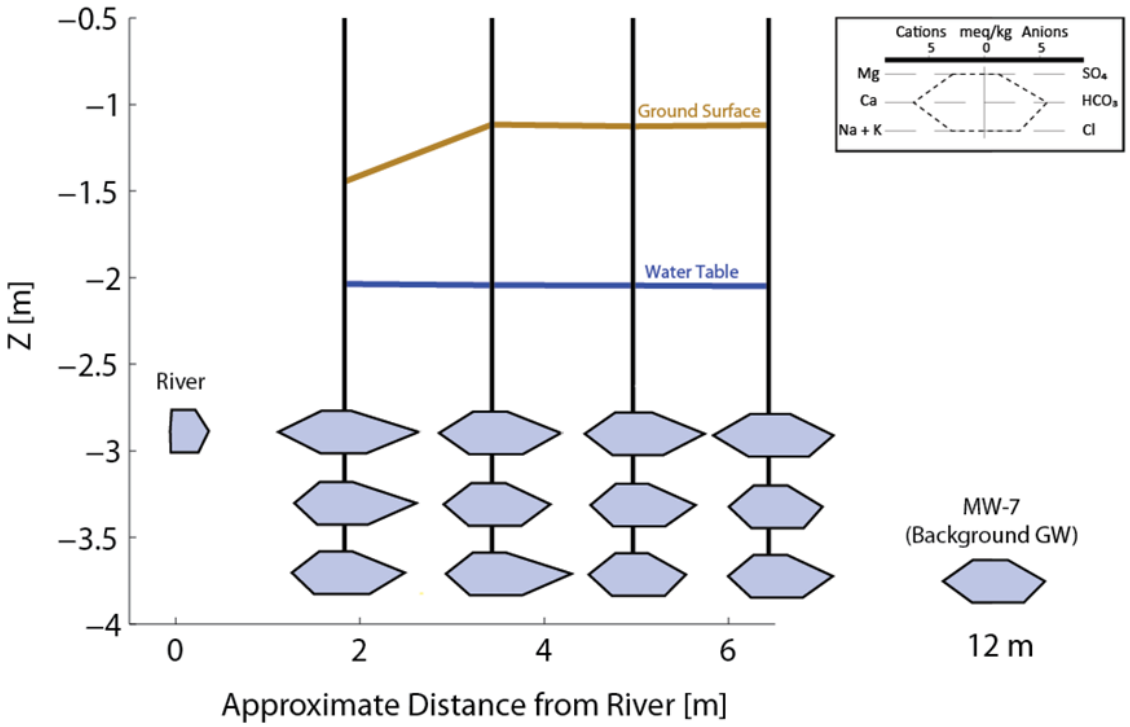

Figure 20: Stiff diagrams for river, sampling wells, and background groundwater.

3.4: IS NITRATE FROM INFILTRATING RIVER WATER DENITRIFIED IN THE BANK?

To examine patterns of nitrate removal within the bank, we plotted the nitrate to chloride concentration ratio versus distance from the river (Figure 21). By plotting the ratio of nitrate and an assumed conservative species, we hope to accentuate nitrate patterns. If nitrate removal is occurring in the bank, we would expect to observe a removal trend, in which high nitrate concentrations eventually decrease. If nitrate were being added from the groundwater, the opposite trend would be expected. However, neither trend is observed within the bank. High nitrate concentrations in the river decrease immediately at the bank. This suggests that a minimal volume of nitrogen-rich surface water is entering the bank environment. Nitrate appears to be acting conservatively because bank concentrations are uniform and low.

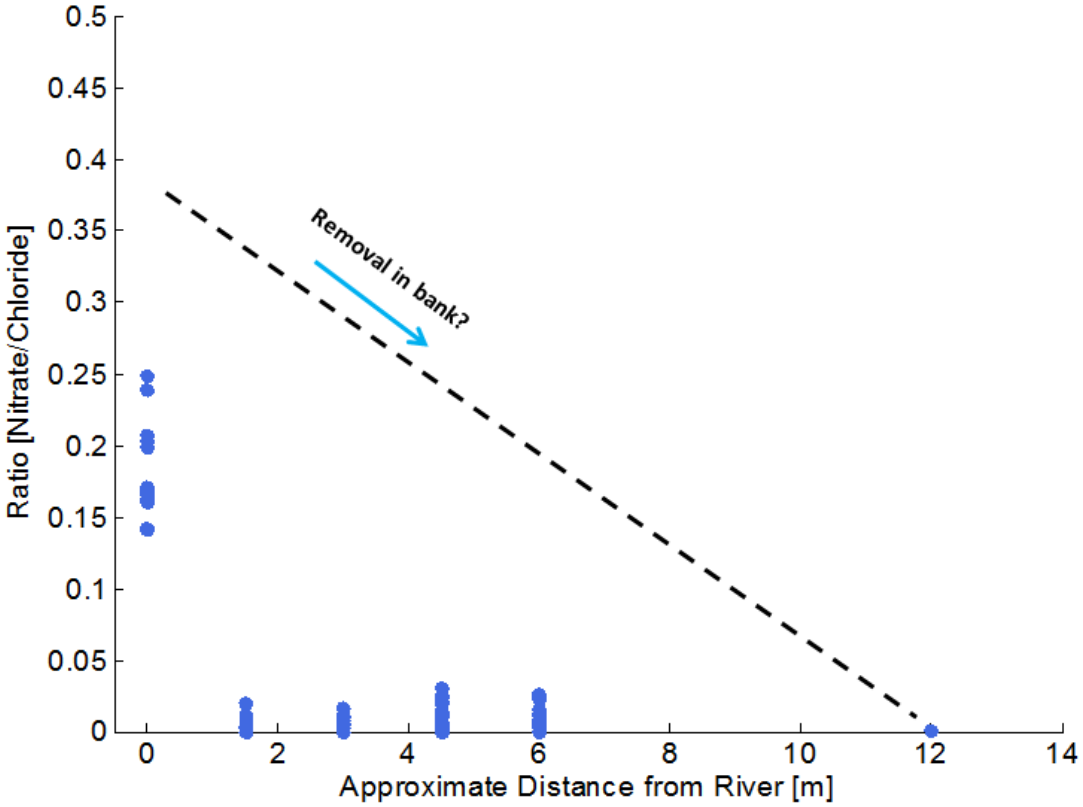

Figure 21: Ratio of nitrate/chloride versus distance in the bank. An abrupt drop-off in nitrate is observed, rather than a gradual decrease.

3.5: PREDICTING THE EFFECTS OF A SHIFTING STAGE: PARTICLE TRACKING AND MODELING GRADIENTS

Given the hydraulic conductivity of the bank material and the measured hydraulic gradients, an equation for average linear flow velocity (adapted from Darcy's Law) can be used to predict flow into the bank. The formula for particle velocity (v) is:

$$v = -\frac{K}{n_e}\frac{dh}{dl} \qquad (10)$$

where K represents the hydraulic conductivity in meters/day, $\frac{dh}{dl}$ is the difference in head divided by the horizontal distance, and n_e is porosity.

At Hornsby Bend, the bank region has an estimated porosity of 0.25 and a hydraulic conductivity of 2.25 meters/day (Sawyer et al., 2009).

Estimating that the peak stage occurs for approximately three hours, we can calculate the distance into the bank that a parcel of river water would be expected to travel for a range of gradients. According to this method, the head gradient (dh/dl) measured during this sampling period (0.08 meters over 1.8 meters) would transport a parcel of river water 0.05 meters into the bank. A head gradient of 1 meter over a 1.8 meter distance (similar to 2010 conditions), would drive river water 0.625 meters into the bank during the same three-hour peak stage. Given this method of estimation, a head gradient or pulse amplitude of ~2.88 meters would be required for river water to infiltrate the first transect of sampling wells (approximately 1.8 meters from the river).

A MATLAB simulation (adapted from Sawyer et al., 2009) was also used to model pulses of varying magnitudes and the head gradients that they would likely produce in the bank. This model took into account estimated aquifer properties such as hydraulic conductivity (K) and specific yield (S_y) and used a sine function to mimic the river fluctuations caused by a pulse. By adjusting the amplitude of the sine function, we can observe the head gradients that various amplitudes would be expected to produce. While this model is simplified in that it assumes a homogeneous aquifer material and

precisely sinusoidal stage behavior, it provides a general indication of the system's response to variable river fluctuations.

When modeling the August 2013 case (amplitude=0.08 m), slight perturbations in hydraulic head are seen approximately 2 meters into the bank. With amplitudes of 0.5 and 1 meter, the same degree of perturbation is seen approximately 8 and 12 meters into the bank, respectively (Figures 22 and 23).

While a large amplitude pulse is required to transport river water into our sampling wells, gradients and physical movement in the bank are expected to occur under even minor fluctuations.

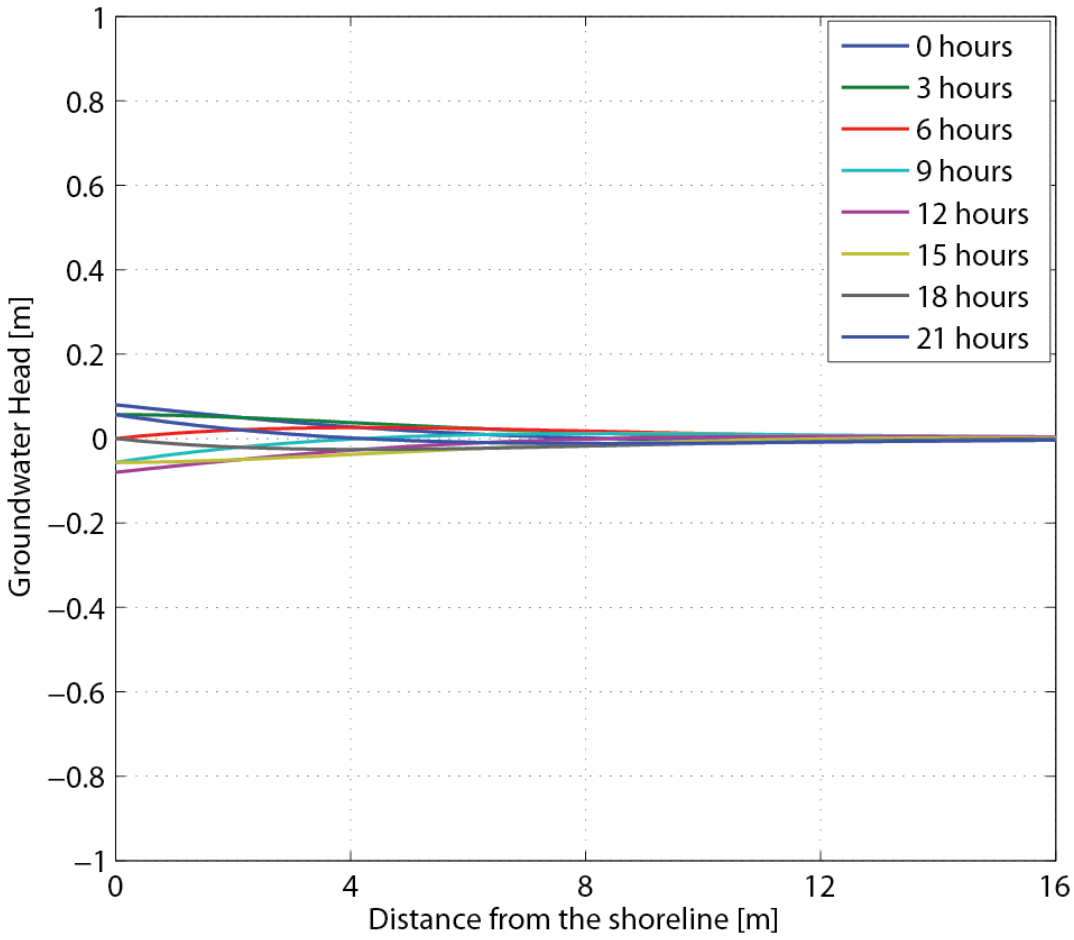

Figure 22: Modeled head gradients in the bank with a 0.08 meter amplitude pulse (similar to what was measured during the August 2013 sampling event).

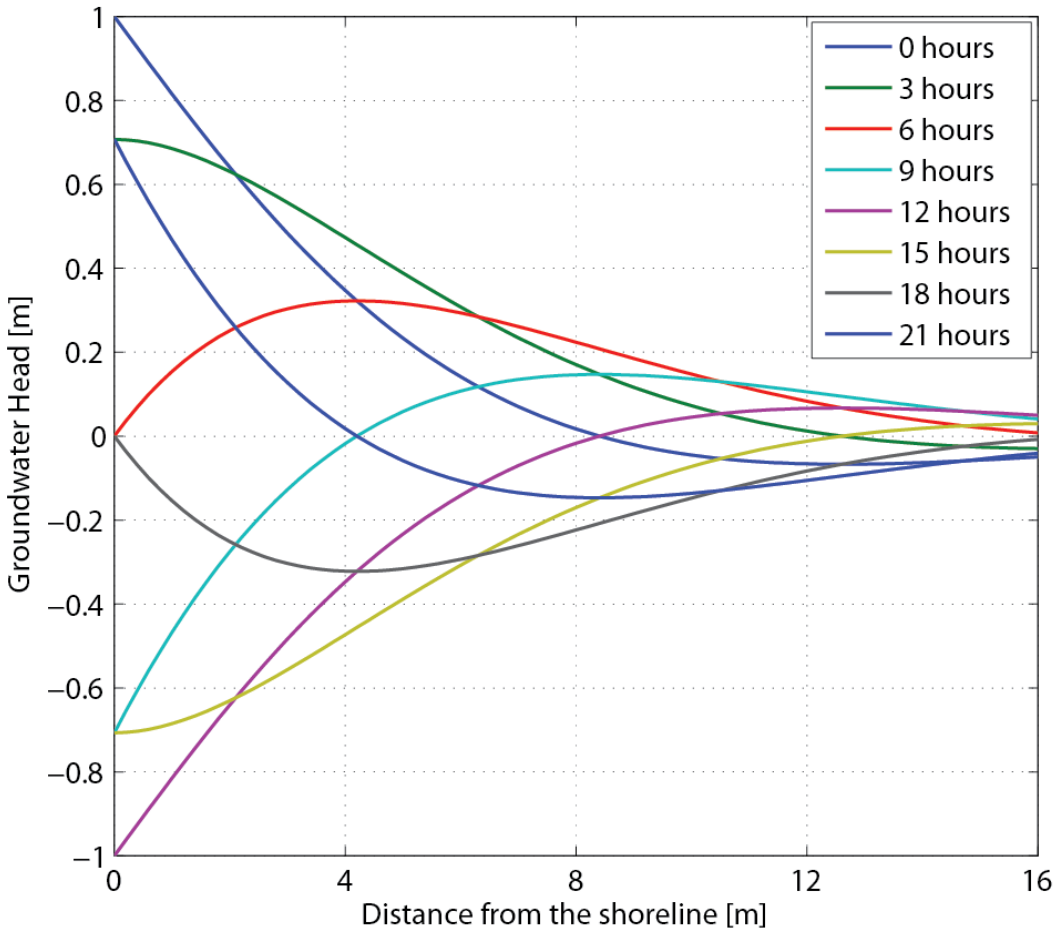

Figure 23: Modeled head gradients in the bank with a 1.0 meter amplitude pulse (similar to August 2010 behavior).

Chapter 4: Summary and Conclusions

The regulation of the LCR creates a dynamic system, in which the management regime (and water level fluctuations) can vary dramatically. This study captured a 16-centimeter change in river stage, which represents muted low-flow conditions for this setting. Under these low-flow conditions, treated wastewater effluent significantly impacts nitrate concentrations in the river. Chemical analysis of bank samples collected over 24 hours revealed abundant organic carbon and a suboxic redox environment. In combination with an influx of nitrate-rich surface water, the bank environment could represent a biogeochemical "hotspot", where conditions are favorable for denitrification. Yet due to the minimum-stage conditions and muted fluctuations measured/observed during this sampling event, surface water infiltration into the bank was minor. The hydraulic gradient was driving surface water toward the bank for the first six hours of the study, but fluxes were not large enough to promote abundant groundwater/surface-water mixing. DIC and chloride distributions, a chloride and stable isotope binary mixing model, and major-ion stiff diagrams offer additional support for two primarily independent systems. Lacking an adequate contribution of nitrate within the system, nitrate removal was not observed within the bank.

The conditions captured here portray a predominantly baseflow/groundwater fed river. Consequently, a pulse causing a 16-centimeter change in stage is not large enough to cause significant groundwater/surface-water interaction in the bank.

Given the normal variations of the LCR and regulated rivers in general, conditions will likely return to higher magnitude dam releases and corresponding hyporheic fluxes. The low-flow biogeochemical conditions captured in this study will provide a useful comparison for more dynamic conditions expected in the future.

Appendix

Sample	Na (mg/L)	K (mg/L)	Ca (mg/L)	Mg (mg/L)	HCO3- (mg/L)	Cl- (mg/L)	SO4- (mg/L)	NO3- (mg/L)	Sum of cations	Sum of anions	Charge balance errror
816-5P-RW	42.67	0.04	38.04	22.08	159.07	53.90	54.46	14.23	5.57	5.49	0.73
817-1A-1S	63.15	0.06	158.30	31.95	612.66	98.05	40.32	0.77	13.28	13.66	-1.43
816-9P-1S	60.08	0.06	152.99	31.04	609.49	82.45	40.32	0.77	12.80	13.17	-1.41
816-7P-1S	60.22	0.06	150.87	31.58	566.85	89.63	40.32	0.77	12.75	12.67	0.30
817-9A-1M	74.32	0.07	121.86	36.41	576.73	100.77	42.55	0.20	12.31	13.19	-3.43
816-3P-1D	81.46	0.08	127.48	36.99	543.71	106.71	44.48	0.50	12.95	12.86	0.36
816-11A-2S	76.60	0.08	141.16	35.67	545.98	107.88	57.71	0.43	13.31	13.20	0.42
816-9A-2M	79.12	0.08	131.31	38.85	579.28	101.51	42.91	0.35	13.19	13.26	-0.25
817-5A-2D	76.90	0.08	127.41	37.53	568.24	102.88	39.79	0.36	12.79	13.05	-1.00
817-9A-3S	74.13	0.07	133.15	36.07	565.55	100.76	70.40	2.47	12.84	13.62	-2.95
816-3P-3M	75.38	0.00	125.93	35.76	555.30	99.84	43.87	0.30	12.51	12.84	-1.31
817-9A-3M	73.07	0.07	120.81	36.03	576.01	105.46	43.87	0.30	12.17	13.34	-4.56
816-3P-3D	76.97	0.08	125.96	37.31	532.86	102.52	41.27	0.34	12.71	12.49	0.85
817-5A-4S	80.73	0.08	158.17	41.80	573.47	128.96	67.94	3.50	14.85	14.51	1.14
816-11P-4M	75.80	0.08	123.03	37.87	552.83	102.74	45.18	0.33	12.55	12.91	-1.39
816-3P-4D	77.88	0.08	128.24	38.29	540.98	98.67	43.24	0.28	12.94	12.56	1.50
816-11P-4D	76.55	0.08	124.72	38.06	528.77	99.27	43.24	0.28	12.69	12.37	1.25
816-11A-MW7	72.98	0.07	135.87	38.40	562.40	106.27	50.01	0.10	13.12	13.26	-0.55

Table A1: Charge balance error for a subset of samples. Bicarbonate calculated from measured DIC. Sample numbering scheme refers to date (8/16 or 8/17, 2013), time (a.m. or p.m.) and well number and depth (shallow, mid, deep).

Time Series of Nitrate Concentration

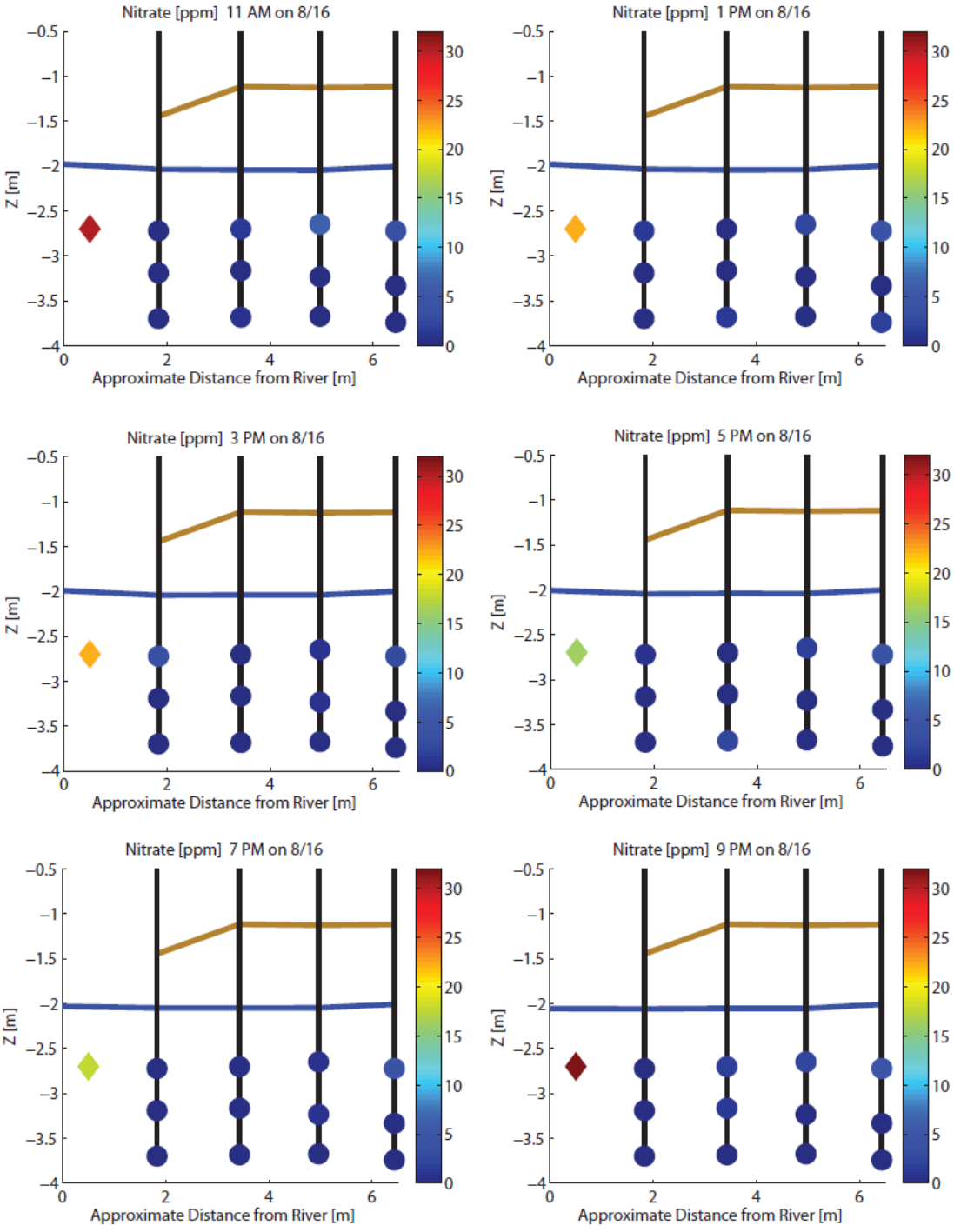

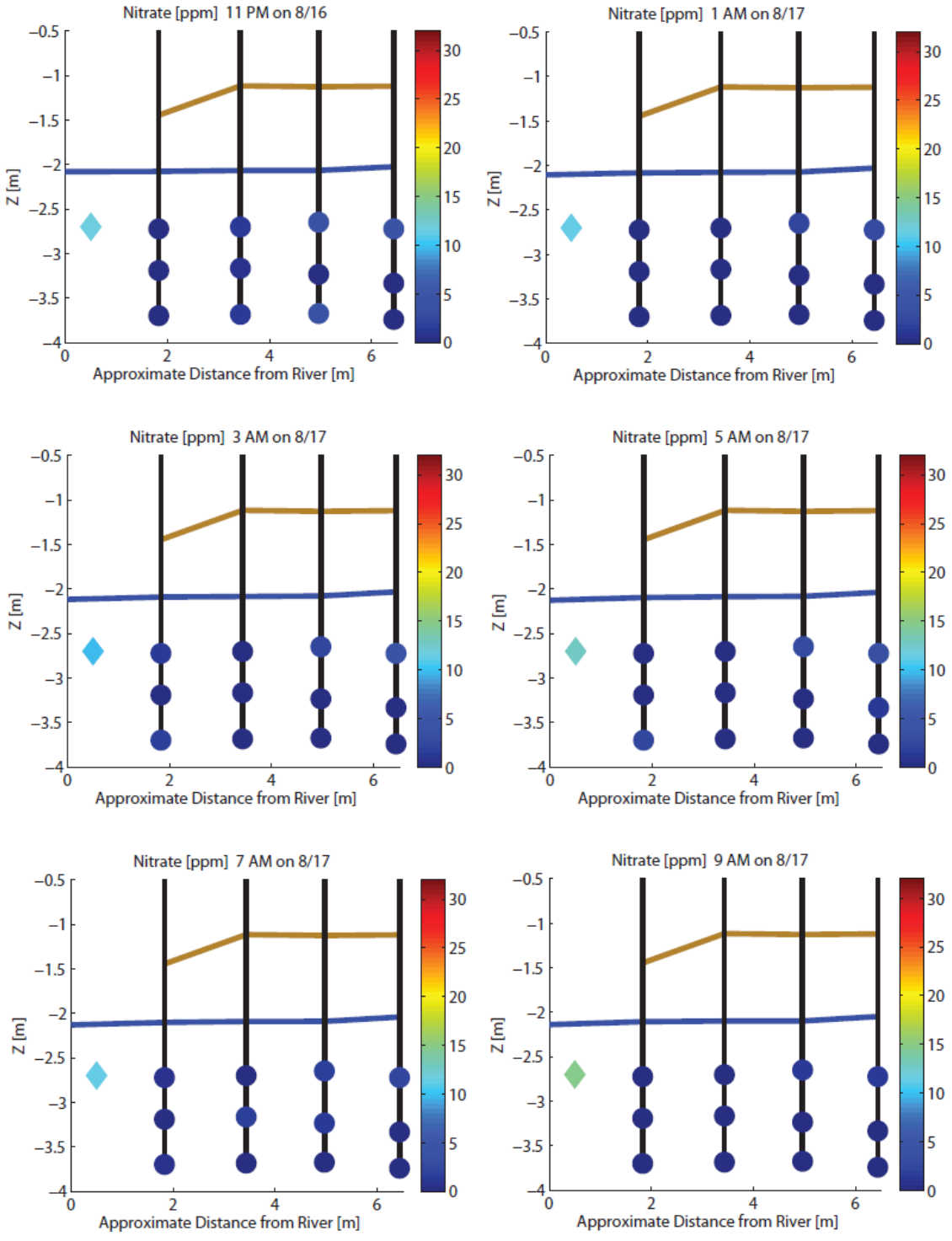
Nitrate [ppm] 11 PM on 8/16
Nitrate [ppm] 1 AM on 8/17
Nitrate [ppm] 3 AM on 8/17
Nitrate [ppm] 5 AM on 8/17
Nitrate [ppm] 7 AM on 8/17
Nitrate [ppm] 9 AM on 8/17
Z [m]
Approximate Distance from River [m]

Time Series of DOC Concentration

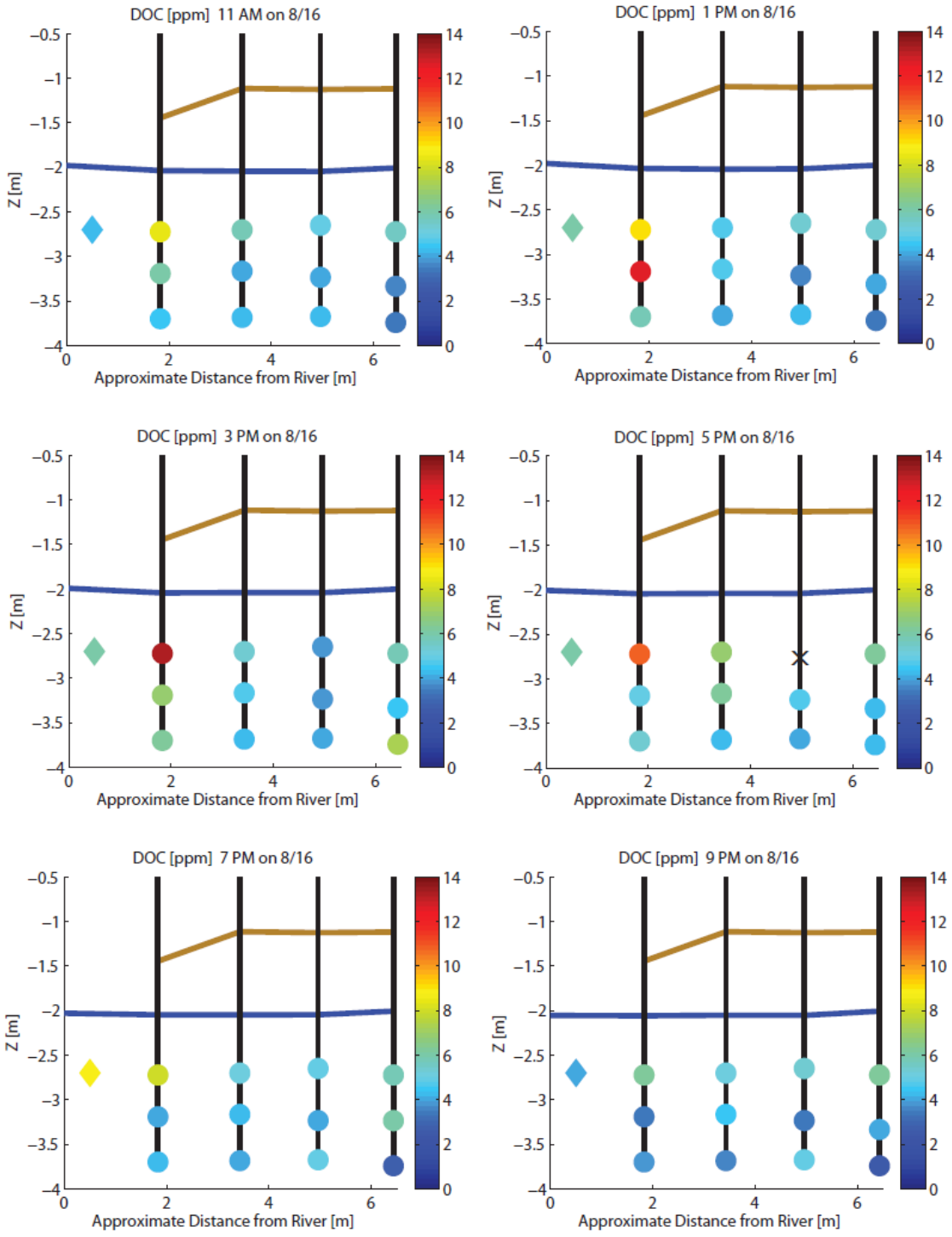

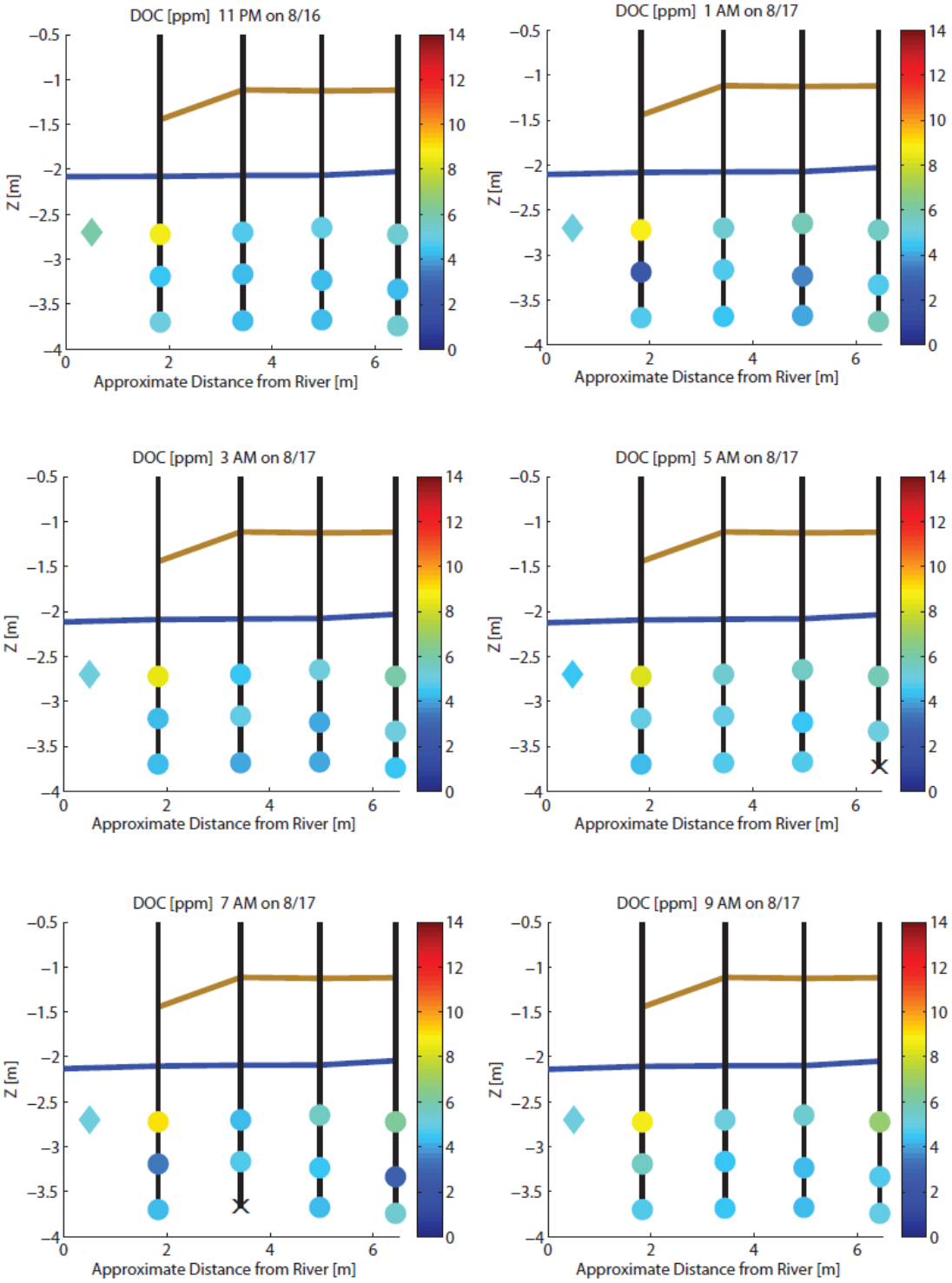
DOC [ppm] 11 PM on 8/16
DOC [ppm] 1 AM on 8/17
DOC [ppm] 3 AM on 8/17
DOC [ppm] 5 AM on 8/17
DOC [ppm] 7 AM on 8/17
DOC [ppm] 9 AM on 8/17
Z [m]
Approximate Distance from River [m]

Time Series of DIC Concentration

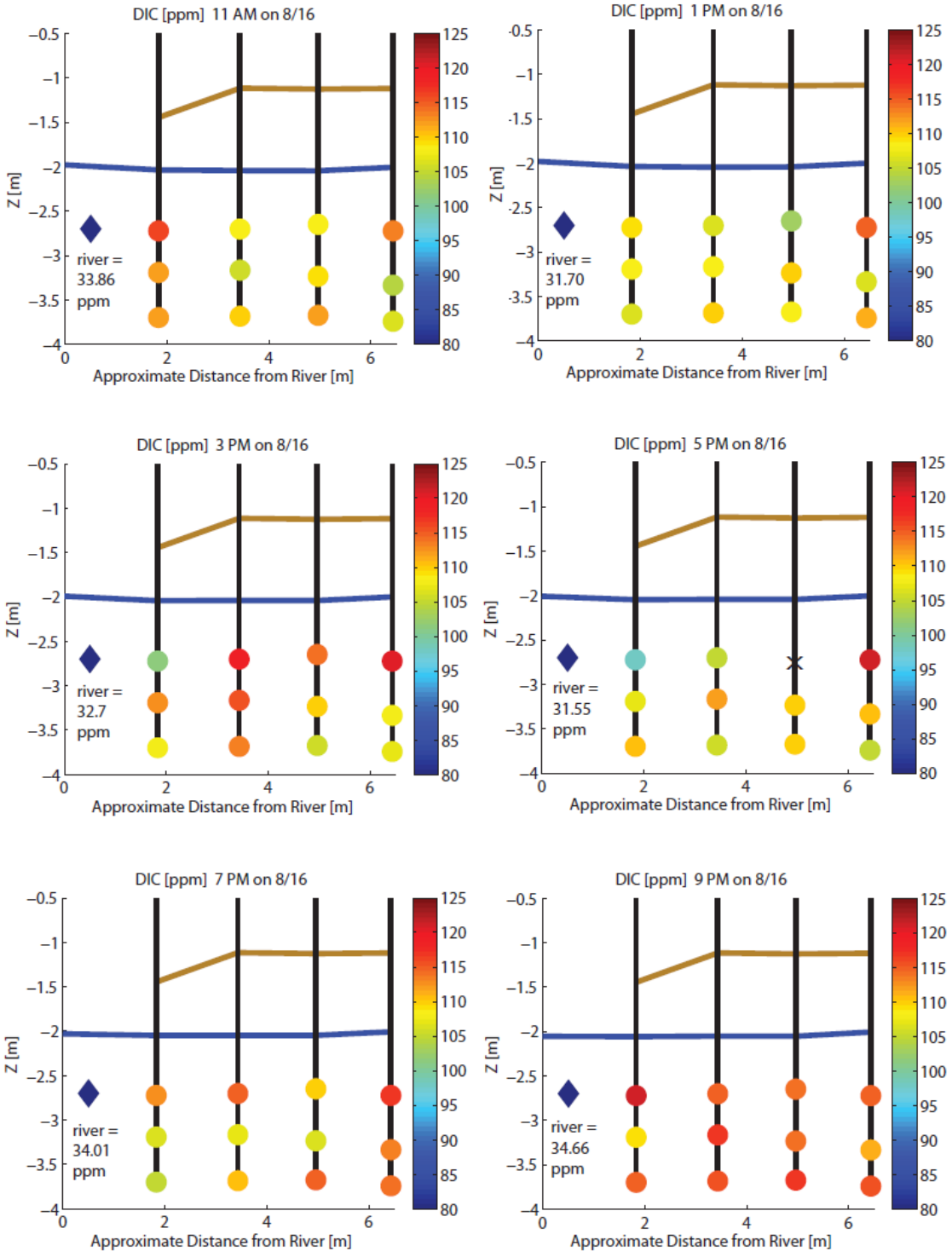

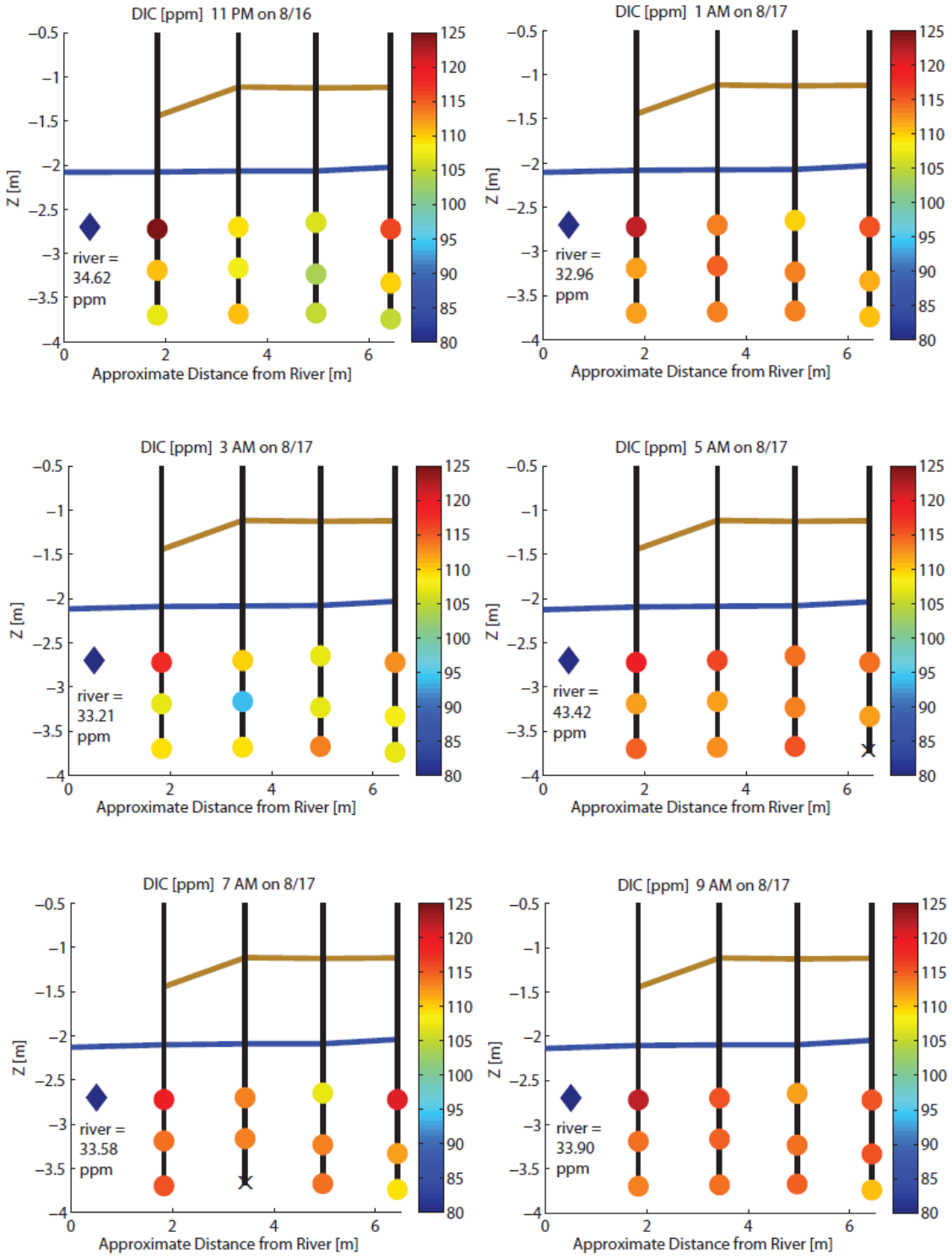
DIC [ppm] 11 PM on 8/16
river = 34.62 ppm
DIC [ppm] 1 AM on 8/17
river = 32.96 ppm
DIC [ppm] 3 AM on 8/17
river = 33.21 ppm
DIC [ppm] 5 AM on 8/17
river = 43.42 ppm
DIC [ppm] 7 AM on 8/17
river = 33.58 ppm
DIC [ppm] 9 AM on 8/17
river = 33.90 ppm
Z [m]
Approximate Distance from River [m]

Time Series of Chloride Concentration

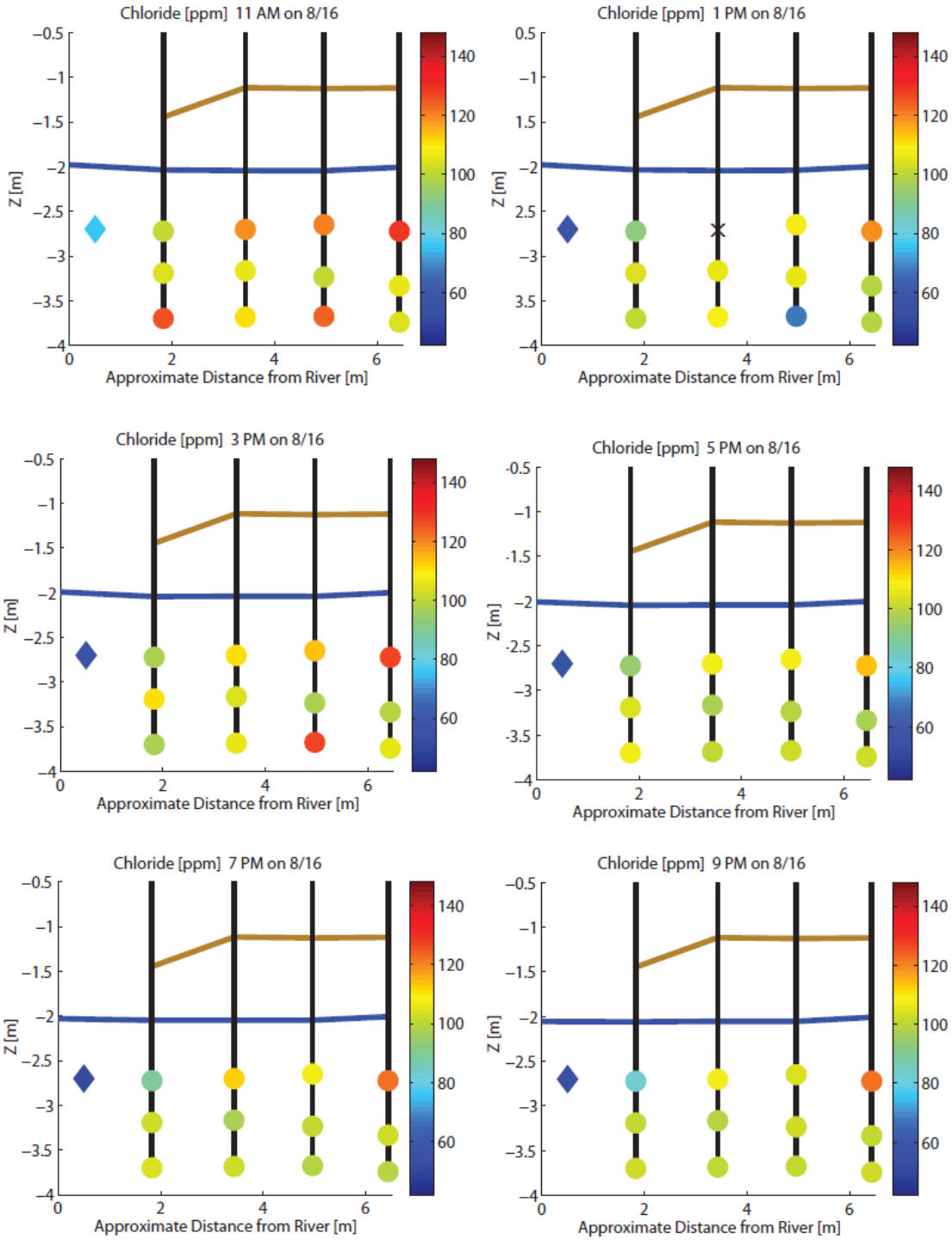

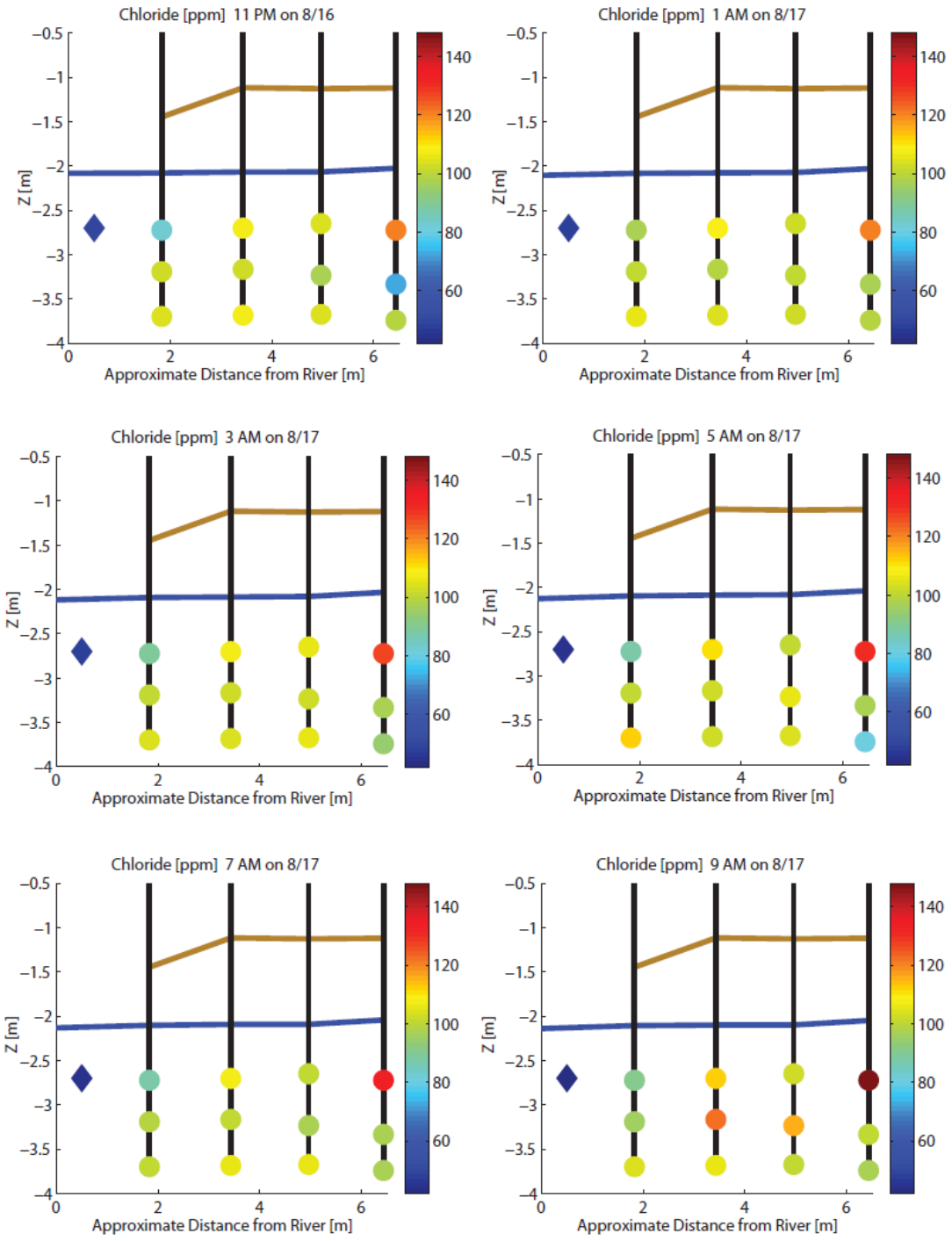

Table A2: Time series of each analyte during 24-hour sampling period.

Well		d18O	dD drift-corrected	d18O raw stdev	dD raw stdev
1M	8/17/13 9:00 AM	0.38	0.2	0.04	0.27
1M	8/17/13 5:00 AM	0.39	0.2	0.01	0.07
1M	8/16/13 9:00 PM	0.43	0.0	0.01	0.07
1M	8/16/13 1:00 PM	0.59	0.1	0.05	0.15
1M	8/17/13 1:00 AM	0.61	0.3	0.04	0.16
1M	8/16/13 5:00 PM	0.63	0.1	0.06	0.13
2M	8/16/13 1:00 PM	0.36	0.0	0.07	0.29
2M	8/16/13 9:00 PM	0.39	0.3	0.05	0.21
2M	8/17/13 5:00 AM	0.42	0.0	0.04	0.14
2M	8/17/13 1:00 AM	0.50	0.3	0.03	0.17
2M	8/17/13 9:00 AM	0.52	0.1	0.02	0.11
2M	8/16/13 5:00 PM	0.55	0.2	0.04	0.15
3M	8/17/13 9:00 AM	0.30	-0.2	0.05	0.20
3M	8/17/13 5:00 AM	0.35	-0.4	0.05	0.18
3M	8/16/13 5:00 PM	0.45	0.1	0.04	0.17
3M	8/16/13 9:00 PM	0.49	0.2	0.07	0.19
3M	8/16/13 1:00 PM	0.49	0.2	0.04	0.25
3M	8/17/13 1:00 AM	0.53	-0.1	0.05	0.07
MW-7	8/16/13 11:00 AM	-0.09	-2.3	0.09	0.11
RW	8/17/13 9:00 AM	0.37	0.5	0.03	0.07
RW	8/17/13 5:00 AM	0.45	0.5	0.06	0.10
RW	8/16/13 1:00 PM	0.53	0.1	0.06	0.08
RW	8/17/13 1:00 AM	0.55	0.6	0.04	0.15
		d18O	dD drift-corrected	d18O raw stdev	dD raw stdev
Duplicates					
1M	8/17/13 9:00 AM	0.40	0.0	0.04	0.10
2M	8/17/13 1:00 AM	0.43	0.0	0.04	0.07
3M	8/16/13 1:00 PM	0.39	-0.1	0.05	0.14
3M	8/16/13 9:00 PM	0.42	0.0	0.07	0.15
RW	8/17/13 5:00 AM	0.32	0.3	0.05	0.05
RW	8/16/13 9:00 PM	0.41	0.3	0.03	0.20
RW	8/16/13 5:00 PM	0.49	0.6	0.06	0.18

Table A3: Stable Isotope values

Bicarbonate [ppm as HCO3-]				
Calculated from DIC concentration and pH				
Well	**Date**	**Time**	**[ppm]**	
RW	16-Aug	5P	159.1	
1S	16-Aug	7P	566.8	
1S	16-Aug	9P	609.5	
1S	17-Aug	1A	612.7	
1S	17-Aug	9A	613.9	
1M	17-Aug	9A	576.7	
1D	16-Aug	3P	543.7	
2S	16-Aug	11A	546.0	
2M	17-Aug	9A	579.3	
2D	17-Aug	5A	568.2	
3S	17-Aug	9A	565.5	
3M	16-Aug	3P	555.3	
3M	17-Aug	9A	576.0	
3D	16-Aug	3P	532.9	
4S	17-Aug	5A	573.5	
4M	16-Aug	11P	552.8	
4D	16-Aug	3P	541.0	
4D	16-Aug	11P	528.8	
MW7	16-Aug	11A	562.4	

Table A4: Bicarbonate values

Dissolved Oxygen in mg/L		
	Well	**[mg/L]**
	1S	dry
	2S	dry
	3S	dry
	4S	dry
	1M	1.3
	2M	0.8
	3M	1.4
	4M	1.1
	1D	1.2
	2D	0.8
	3D	0.7
	4D	0.6

Table A5: Dissolved Oxygen

Dissolved Inorganic Carbon (DIC) [mg/L]												
Well	**11:00 AM**	**1:00 PM**	**3:00 PM**	**5:00 PM**	**7:00 PM**	**9:00 PM**	**11:00 PM**	**1:00 AM**	**3:00 AM**	**5:00 AM**	**7:00 AM**	**9:00 AM**
1S	116.4	109.4	101.3	98.0	112.4	120.9	124.5	121.5	117.5	118.7	119.3	121.8
2S	108.3	106.6	119.0	105.1	114.7	114.5	108.9	113.1	109.8	116.0	113.3	115.6
3S	108.3	103.1	113.9	na	109.7	113.8	106.4	109.7	107.0	114.3	106.9	112.2
4S	113.3	115.1	120.3	121.1	116.6	114.8	115.9	115.3	112.5	113.8	120.5	115.2
1M	112.2	108.2	112.4	106.9	106.1	109.1	110.4	112.1	107.0	112.2	114.1	114.4
2M	105.5	108.2	115.5	112.2	107.2	116.6	107.8	114.6	93.6	112.0	113.3	114.9
3M	109.4	110.1	110.2	110.0	106.3	113.9	103.3	113.1	106.7	113.6	113.3	114.3
4M	104.0	106.6	107.6	110.6	113.2	111.3	109.7	111.3	107.5	112.2	112.2	115.8
1D	111.7	106.4	107.9	110.5	104.7	114.8	107.3	112.2	109.3	114.8	115.2	113.6
2D	109.9	109.8	113.4	106.0	110.5	115.5	110.5	113.3	108.9	112.7	na	114.3
3D	111.9	108.6	105.7	109.7	114.9	116.9	104.8	113.2	113.3	115.8	114.2	114.6
4D	106.4	111.5	107.3	104.8	113.8	115.5	104.9	110.8	106.9	na	108.9	110.8
River	33.9	31.7	32.7	31.6	34.0	34.7	34.6	33.0	33.2	43.4	33.6	33.9
MW7												
	816-11 am	111.6										
Well	Average	Standard deviation	% Relative standard deviation			Quality Control						
1S	115.1577678	8.351009	7.3			Date	Well	Time	mg/L			
2S	112.0765128	4.260769	3.8			16-Aug	4M	11P	109.6			
3S	109.5672203	3.646969	3.3			16-Aug	Field Blank	1:30P	3.2			
4S	116.1910517	2.894556	2.5			17-Aug	2D	5A	114.8			
1M	110.4155933	2.899959	2.6			17-Aug	FB	5A	2.3			
2M	110.1261097	6.352895	5.8			25-Sep	MW7	2P	118.0			
3M	110.3399292	3.513755	3.2			25-Sep	MW7	2P	116.6			
4M	110.1773789	3.256207	3.0									
1D	110.6863483	3.585162	3.2									
2D	111.3480433	2.772217	2.5									
3D	111.9689172	3.922253	3.5									
4D	109.2399648	3.557739	3.3									
River	34.17905528	3.074875	9.0									
MW7	111.5577333											

Table A6: Dissolved Inorganic Carbon

Dissolved Organic Carbon (DOC) [mg/L]												
Well	**11:00 AM**	**1:00 PM**	**3:00 PM**	**5:00 PM**	**7:00 PM**	**9:00 PM**	**11:00 PM**	**1:00 AM**	**3:00 AM**	**5:00 AM**	**7:00 AM**	**9:00 AM**
1S	8.3	9.1	13.2	10.8	8.1	6.3	8.6	8.8	8.5	8.2	9.1	8.7
2S	5.9	4.8	5.3	7.0	5.1	5.1	4.8	5.3	4.5	5.4	4.2	5.2
3S	4.9	5.3	3.9	na	4.9	5.4	4.9	5.9	5.1	5.6	5.5	5.3
4S	5.5	5.3	5.7	6.3	5.8	6.3	5.3	5.5	6.0	5.7	6.2	7.0
1M	5.9	12.5	6.8	4.9	4.0	3.4	4.6	2.3	4.2	5.0	3.3	5.6
2M	4.0	4.7	4.8	6.3	4.3	4.6	4.2	4.6	4.9	4.8	4.7	4.5
3M	4.0	3.7	3.8	4.7	4.1	3.4	4.2	3.6	4.0	4.4	4.5	4.2
4M	3.6	4.1	4.6	4.3	6.0	4.1	4.2	4.8	5.1	5.1	2.8	4.8
1D	4.5	5.9	6.2	5.4	4.3	3.8	5.2	4.7	4.2	4.3	4.3	4.6
2D	4.2	4.0	4.4	4.2	4.0	3.7	4.2	4.5	4.0	4.6	na	4.5
3D	4.2	4.2	4.2	4.0	4.9	4.9	4.3	4.1	4.0	4.6	4.2	4.4
4D	3.4	3.5	7.2	4.2	2.8	2.5	5.3	5.8	4.4	na	5.4	5.0
River	4.2	6.1	6.0	6.1	8.9	4.1	5.9	5.1	5.1	4.6	5.2	5.1
MW7												
	816-12pm	10.8										
	925-2pm	2.8										
	925-2pm	3.4										

Well	Average	Standard deviation	% Relative standard deviation
1S	9.0	1.7	18.6
2S	5.2	0.7	13.4
3S	5.2	0.5	10.0
4S	5.9	0.5	8.3
1M	5.2	2.6	50.0
2M	4.7	0.6	12.0
3M	4.1	0.4	9.5
4M	4.4	0.8	18.3
1D	4.8	0.7	15.3
2D	4.2	0.3	6.4
3D	4.3	0.3	7.5
4D	4.5	1.4	31.6
River	5.5	1.3	23.1
MW7	5.7	4.4	78.2

Quality Control:			
Date	Well	Time	mg/L
16-Aug	1M	11A	5.1
16-Aug	RW	3P	5.3
16-Aug	1S	3P	6.2
16-Aug	2S	3P	4.3
16-Aug	1M	3P	3.8
16-Aug	2D	3P	3.5
16-Aug	4S	5P	5.1
16-Aug	3D	7P	4.0
16-Aug	2S	7P	4.1
16-Aug	RW	7P	5.7
16-Aug	4S	9P	4.6
16-Aug	3S	9P	4.2
16-Aug	4M	11P	4.2
17-Aug	2D	1A	3.8
17-Aug	1A	1A	3.9
17-Aug	2D	5A	4.5
17-Aug	2D	5A	3.9
17-Aug	3D	5A	3.1
17-Aug	FB	5A	1.1
17-Aug	3M	5A	3.5
17-Aug	4S	7A	3.9
17-Aug	3S	7A	4.7
17-Aug	RW	7A	4.6
17-Aug	2M	7A	3.4
17-Aug	2S	9A	4.6
17-Aug	3S	9A	4.5
17-Aug	3M	9A	3.6
17-Aug	4S	9A	5.0

Table A7: Dissolved Organic Carbon

Nitrate as NO3- [mg/L]												
Well	**11:00 AM**	**1:00 PM**	**3:00 PM**	**5:00 PM**	**7:00 PM**	**9:00 PM**	**11:00 PM**	**1:00 AM**	**3:00 AM**	**5:00 AM**	**7:00 AM**	**9:00 AM**
1S	0.0	1.2	3.4	1.0	0.0	0.4	0.0	0.0	1.3	0.0	0.8	0.0
2S	1.0	0.0	0.0	0.5	0.0	1.8	1.2	0.4	0.0	0.0	0.4	0.0
3S	6.4	2.2	0.6	1.6	0.9	2.0	3.9	2.1	2.1	3.0	1.8	1.3
4S	3.4	4.1	2.7	4.4	4.2	4.9	4.2	2.7	4.4	3.0	2.4	1.4
1M	0.0	0.0	0.0	0.5	0.4	0.5	0.0	0.4	0.4	0.0	0.0	0.1
2M	0.0	0.0	0.0	0.4	0.0	1.2	0.7	0.0	0.0	0.0	1.6	0.0
3M	0.0	0.1	0.8	0.4	0.5	0.0	0.5	0.0	0.0	0.0	1.0	0.0
4M	0.4	0.0	0.0	0.0	0.0	0.0	0.4	0.0	0.0	1.0	0.0	0.0
1D	0.0	0.0	0.0	0.0	0.0	0.0	0.0	0.0	1.8	2.2	0.5	0.0
2D	0.6	1.2	0.0	2.4	0.4	0.0	1.5	0.0	0.0	0.0	0.0	0.0
3D	0.0	0.0	0.0	0.0	0.0	0.0	3.8	0.0	0.0	0.0	0.0	0.0
4D	0.0	1.9	0.0	0.0	0.0	0.0	0.4	0.0	0.4	0.5	0.0	0.0
River	30.2	22.1	22.5	16.0	17.7	11.4	11.5	11.5	9.7	13.0	11.4	14.8
MW7	816-11am	trace										
	925-2pm	5.4										
	925-2pm	2.8										
Well	Average	Standard deviation	% Relative standard deviation			Replicates						
1S	0.7	1.0	148.7				Well	Time	mg/L	Date		
2S	0.4	0.6	132.5				1S	9P	0.4	16-Aug		
3S	2.3	1.6	66.6				2S	7A	0.4	17-Aug		
4S	3.5	1.1	30.2				2S	1A	0.0	17-Aug		
1M	0.2	0.2	113.7				3S	5A	3.0	17-Aug		
2M	0.3	0.5	168.4				4S	5A	3.0	17-Aug		
3M	0.3	0.4	132.0				4S	7P	4.2	16-Aug		
4M	0.2	0.3	206.3				1M	5A	0.0	17-Aug		
1D	0.4	0.8	207.1				3M	1P	trace	16-Aug		
2D	0.5	0.8	154.5				4M	5A	1.1	17-Aug		
3D	0.3	1.1	346.0				4M	11P	1.1	16-Aug		
4D	0.3	0.5	203.0				2D	1A	0.0	17-Aug		
River	16.0	6.2	38.6				2D	7A	0.0	17-Aug		
							3D	5A	0.0	17-Aug		
							3D	1A	0.0	17-Aug		
							RW	7A	11.2	17-Aug		
							RW	5P	16.1	16-Aug		
							RW	5A	12.4	17-Aug		
							RW	5A	12.9	17-Aug		
							4D	3A	1.0	17-Aug		

Table A8: Nitrate data

Nitrite:				
All values zero except for measurements below:				
	Well	Time	mg/L	Date
	RW	1A	0.3	17-Aug
	RW	3A	0.3	17-Aug
	RW	11P	0.3	16-Aug
	RW	7A	0.3	17-Aug
	RW	7A	0.3	17-Aug
	RW	5P	0.3	16-Aug
	RW	5P	0.3	16-Aug
	RW	9P	0.4	16-Aug
	RW	1P	0.4	16-Aug
	RW	3P	0.1	16-Aug
	RW	5A	trace	17-Aug
	RW	5A	trace	17-Aug
	RW	11A	0.3	16-Aug
	MW7	2P	0.1	25-Sep

Table A9: Nitrite data

Chloride [mg/L]												
Well	**11:00 AM**	**1:00 PM**	**3:00 PM**	**5:00 PM**	**7:00 PM**	**9:00 PM**	**11:00 PM**	**1:00 AM**	**3:00 AM**	**5:00 AM**	**7:00 AM**	**9:00 AM**
1S	101.2	92.7	96.8	94.3	89.6	82.5	83.2	98.0	89.4	86.9	88.2	91.5
2S	119.5	na	111.0	108.2	112.8	107.9	107.7	108.6	108.1	110.6	107.1	112.0
3S	120.1	107.7	113.7	106.7	107.6	104.4	104.6	101.8	105.0	101.6	100.8	103.2
4S	129.6	119.3	127.2	113.4	122.5	122.0	120.7	120.6	127.7	130.8	133.4	147.3
1M	104.5	103.7	111.2	103.6	101.7	100.8	103.2	100.7	101.6	100.1	99.8	96.1
2M	105.8	105.9	103.4	97.9	97.2	99.9	102.6	99.0	102.1	101.7	101.5	122.1
3M	100.0	105.8	97.9	99.8	100.5	102.1	97.5	101.1	102.1	105.5	98.1	114.9
4M	105.4	99.8	98.7	97.5	101.9	100.3	72.9	96.8	97.5	97.7	97.4	101.1
1D	125.8	100.6	97.3	106.7	104.2	102.1	103.6	105.6	103.6	112.4	100.4	103.8
2D	110.7	109.0	106.0	100.2	103.3	100.7	107.4	104.2	103.4	102.9	106.4	105.7
3D	124.5	67.4	126.6	102.5	99.8	100.5	104.8	102.6	105.5	103.6	105.3	100.3
4D	104.6	98.7	105.2	101.7	99.6	102.6	99.3	99.7	93.7	80.2	98.3	97.4
River	76.4	58.4	53.8	53.9	50.8	52.6	49.1	48.4	47.3	43.8	47.0	43.1
MW7	816-11am	106.3										
	925-2pm	92.3										
	925-2pm	109.7										

Well	Average	Standard deviation	% Relative standard deviation			Replicates	Well	Time	mg/L	Date		
1S	91.2	5.8	6.3				1S	9P	81.9	16-Aug		
2S	110.3	3.6	3.3				2S	7A	107.9	17-Aug		
3S	106.4	5.6	5.2				2S	1A	109.6	17-Aug		
4S	126.2	8.7	6.9				3S	5A	101.7	17-Aug		
1M	102.2	3.6	3.5				4S	5A	129.0	17-Aug		
2M	103.3	6.5	6.3				4S	7P	120.0	16-Aug		
3M	102.1	4.8	4.7				1M	5A	99.8	17-Aug		
4M	97.3	8.1	8.3				3M	1P	105.9	16-Aug		
1D	105.5	7.4	7.0				4M	5A	97.8	17-Aug		
2D	105.0	3.2	3.0				1D	3P	107.1	16-Aug		
3D	103.6	14.5	14.0				2D	7A	107.2	17-Aug		
4D	98.4	6.5	6.6				2D	1A	104.8	17-Aug		
River	52.0	8.8	17.0				3D	5A	103.5	17-Aug		
MW7	102.8	9.3	9.0				3D	1A	98.8	17-Aug		
							3D	9A	100.8	17-Aug		
							3D	11A	126.9	16-Aug		
							4D	5P	103.1	16-Aug		
							4D	3A	106.8	17-Aug		
							RW	5A	44.1	17-Aug		
							RW	5A	43.3	17-Aug		
							RW	5P	53.0	16-Aug		
							RW	7A	45.6	17-Aug		
							4M	11P	102.7362	16-Aug		

Table A10: Chloride data

Table A11: Cation data by hour

11AM on 8/16/13														
Well	Li [ppb]	B [ppb]	Na [ppb]	Mg [ppb]	Al [ppb]	Si [ppb]	P [ppb]	Ca [ppb]	Ti [ppb]	V [ppb]	Cr [ppb]	Mn [ppb]	Fe [ppb]	K [ppb]
1S	14.4	138.6	62753.7	32058.7	4.5	14023.2	29.8	150806.5	2.2	5.1	0.3	1022.8	21.6	2054.6
2S	19.8	195.7	76599.2	35666.9	2.5	10482.2	128.9	141163.0	1.6	1.7	bdl	657.5	1302.2	2354.3
3S	19.3	173.7	73544.0	38299.4	bdl	10499.2	36.1	146712.3	1.6	1.3	bdl	588.9	516.6	2665.3
4S	20.6	208.6	77040.3	40848.8	bdl	10778.3	83.1	146842.2	1.7	2.4	bdl	343.0	164.5	3798.1
1M	19.8	204.8	73659.4	35819.9	bdl	9920.3	62.9	121478.7	1.3	2.4	bdl	209.1	49.7	4449.3
2M	20.6	208.0	74746.1	36603.1	6.1	10249.3	56.6	122795.0	1.6	2.6	0.2	249.3	39.4	4838.2
3M	20.8	210.2	74329.8	36825.1	2.0	10193.6	66.2	123505.4	1.4	2.5	bdl	106.9	109.7	4736.3
4M	20.8	210.1	73735.8	38080.1	7.5	10160.6	63.6	122400.2	1.6	2.5	0.5	250.0	232.9	4989.6
1D	20.7	209.6	77379.9	37293.5	bdl	9878.5	43.4	122173.6	1.5	1.7	bdl	2013.2	216.4	5700.1
2D	21.2	210.2	76037.6	37475.8	bdl	9699.7	39.5	121924.8	1.5	2.0	bdl	1502.6	47.5	5509.8
3D	20.5	204.9	74437.6	37154.1	2.7	9663.5	42.4	119398.9	1.3	1.6	0.1	1498.7	109.0	4200.4
4D	20.2	200.8	71990.1	36944.5	3.1	9786.3	59.1	117824.9	1.6	2.0	0.4	547.2	205.2	5387.8
RW	8.3	122.3	50416.3	24135.0	1.7	4444.5	920.1	38562.4	1.5	2.2	0.3	7.0	10.4	6797.4
1PM on 8/16/13														
Well	Li [ppb]	B [ppb]	Na [ppb]	Mg [ppb]	Al [ppb]	Si [ppb]	P [ppb]	Ca [ppb]	Ti [ppb]	V [ppb]	Cr [ppb]	Mn [ppb]	Fe [ppb]	K [ppb]
1S	12.9	131.1	61441.4	31623.4	bdl	15656.2	16.4	161175.9	bdl	1.2	bdl	1553.6	24.0	1912.7
2S	19.2	196.1	76624.6	34801.3	bdl	10274.3	106.1	140140.2	1.3	1.0	bdl	572.0	822.9	2529.3
3S	19.1	190.0	75590.4	36397.2	bdl	10208.7	18.4	142285.5	1.3	3.2	bdl	470.8	119.4	2760.1
4S	21.8	229.3	78773.2	43442.2	2.8	10897.7	92.8	151219.9	1.4	3.5	0.1	363.5	125.4	3893.0
1M	19.6	208.9	77477.1	36465.1	bdl	10404.4	69.2	129459.4	bdl	2.6	bdl	227.9	40.1	4640.3
2M	19.6	206.7	76020.6	36268.6	bdl	10390.7	64.6	126272.1	bdl	2.5	bdl	242.7	26.5	4995.5
3M	20.2	207.7	75396.3	36306.7	bdl	10194.3	61.5	126910.5	1.5	2.1	bdl	113.8	103.2	4759.6
4M	20.2	207.2	74917.9	37918.1	bdl	10427.5	72.3	127282.4	bdl	1.8	0.1	216.1	158.5	5063.7
1D	20.2	208.7	79272.7	36758.1	bdl	9800.8	37.2	125235.1	1.4	1.7	bdl	1948.9	139.0	5846.6
2D	20.3	210.0	79207.7	37497.5	1.8	10372.9	43.6	126879.4	bdl	2.0	0.1	1488.4	47.0	5907.8
3D	20.3	209.3	77129.9	37406.3	bdl	10293.9	47.2	125516.4	bdl	1.2	bdl	1495.9	113.5	5594.5
4D	20.7	208.4	75928.1	37764.9	bdl	10168.2	46.6	125086.2	1.4	2.0	bdl	599.4	165.5	5567.1
RW	8.0	121.3	50278.9	23395.8	bdl	4586.6	909.2	40398.4	bdl	2.1	0.2	8.4	7.1	6786.3
FB	bdl	bdl	bdl	50.4	bdl	bdl	bdl	563.5	bdl	0.0	bdl	bdl	bdl	47.2
3PM on 8/16/13														
Well	Li [ppb]	B [ppb]	Na [ppb]	Mg [ppb]	Al [ppb]	Si [ppb]	P [ppb]	Ca [ppb]	Ti [ppb]	V [ppb]	Cr [ppb]	Mn [ppb]	Fe [ppb]	K [ppb]
1S	12.7	128.2	62232.2	31588.0	bdl	15779.3	25.6	161430.1	bdl	1.3	0.1	1616.3	20.5	1946.6
2S	19.5	202.4	79523.3	36103.5	bdl	10884.9	141.9	146227.9	bdl	0.5	bdl	557.6	716.0	2670.4
3S	19.0	196.4	78037.8	36583.0	bdl	10587.0	47.0	141886.9	bdl	1.4	bdl	373.8	211.1	2742.5
4S	19.8	211.1	78797.9	40589.8	bdl	11198.2	78.5	152812.3	bdl	2.9	bdl	342.7	135.9	3803.8
1M	20.0	208.4	76705.1	36867.0	bdl	10482.7	61.2	130391.7	bdl	2.6	bdl	291.0	38.2	4738.9
2M	20.0	206.5	75670.7	35996.6	bdl	10145.2	58.7	125669.3	1.4	2.4	bdl	264.9	40.1	4925.1
3M	20.1	205.0	75379.8	35759.4	bdl	10108.1	61.3	125929.9	1.4	2.3	bdl	108.6	84.2	4663.0
4M	20.0	211.9	76671.8	38276.0	bdl	10502.4	67.9	128784.7	bdl	1.9	bdl	217.6	148.9	5279.2
1D	19.8	210.3	81464.2	36988.2	bdl	10157.3	41.4	127481.1	bdl	2.2	bdl	1930.4	100.8	5835.3
2D	20.5	210.8	78498.2	37565.8	bdl	10267.7	42.6	127259.7	bdl	2.2	bdl	1499.7	29.7	5742.0
3D	20.5	210.4	76965.1	37310.7	bdl	10093.1	48.7	125964.7	1.2	1.7	bdl	1421.2	93.3	5681.9
4D	20.7	212.0	77879.8	38292.2	bdl	10701.5	53.8	128238.6	bdl	1.9	bdl	599.7	181.7	5718.4
RW	8.1	114.6	47352.4	22962.6	bdl	4525.1	810.2	40702.4	bdl	2.3	bdl	8.2	7.8	6697.5

Table A11 continued: Cation data by hour

5PM on 8/16/13														
Well	Li [ppb]	B [ppb]	Na [ppb]	Mg [ppb]	Al [ppb]	Si [ppb]	P [ppb]	Ca [ppb]	Ti [ppb]	V [ppb]	Cr [ppb]	Mn [ppb]	Fe [ppb]	K [ppb]
1S	13.4	132.2	60457.2	31755.4	bdl	15406.8	19.4	157835.2	2.1	1.7	0.2	1722.1	544.9	1838.1
2S	18.9	197.1	77794.9	35008.2	bdl	10262.0	131.7	139079.1	1.7	0.9	bdl	513.6	614.9	2606.7
3S	19.6	199.8	76196.4	36705.6	bdl	10763.0	61.4	142147.0	bdl	1.5	bdl	364.1	318.0	2809.1
4S	20.5	207.8	78650.2	40315.1	bdl	11007.5	78.4	148400.4	1.7	3.1	bdl	322.9	141.6	3893.3
1M	20.5	207.3	75770.5	36737.5	bdl	10437.6	59.6	127232.4	1.5	2.5	bdl	231.7	35.3	4444.8
2M	20.4	207.0	76363.4	36207.0	3.1	9927.7	56.6	123923.5	1.4	2.6	bdl	265.6	38.0	4955.9
3M	20.0	204.8	76685.8	36143.2	bdl	9986.0	57.7	124301.4	1.3	2.4	bdl	109.4	83.7	4634.9
4M	20.6	207.0	74689.9	37876.1	bdl	10238.6	63.4	124516.0	1.4	1.9	bdl	194.4	160.1	5128.2
1D	20.7	211.5	79877.9	37326.3	bdl	10145.0	37.9	125111.2	1.5	2.0	bdl	1928.4	90.3	5889.8
2D	20.2	211.0	77388.4	37672.0	bdl	10440.2	47.7	127624.4	bdl	2.0	bdl	1511.5	43.6	5779.8
3D	20.4	206.8	77663.8	37397.4	bdl	9590.1	42.6	121882.6	1.3	1.4	bdl	1415.4	94.5	5642.7
4D	20.6	209.2	75476.0	37853.7	bdl	10650.1	52.9	127519.8	bdl	1.7	bdl	599.3	189.1	5504.1
RW	7.7	108.0	42674.5	22082.6	3.1	4075.6	662.5	38043.3	1.4	2.0	bdl	8.5	13.6	6488.6
7PM on 8/16/13														
Well	Li [ppb]	B [ppb]	Na [ppb]	Mg [ppb]	Al [ppb]	Si [ppb]	P [ppb]	Ca [ppb]	Ti [ppb]	V [ppb]	Cr [ppb]	Mn [ppb]	Fe [ppb]	K [ppb]
1S	13.2	129.2	60217.9	31584.0	bdl	15165.5	28.0	150865.3	2.1	2.9	0.1	1242.3	17.9	1886.6
2S	20.0	199.6	77994.2	35728.5	bdl	10770.7	104.5	140295.1	1.6	0.6	bdl	525.0	464.2	2542.1
3S	19.5	191.5	74795.8	36029.8	bdl	10351.3	53.7	138958.0	1.5	1.8	bdl	353.8	314.4	2787.9
4S	19.9	205.0	79345.4	39853.2	bdl	10396.9	75.2	145576.9	1.5	3.4	bdl	296.5	116.3	3818.9
1M	19.9	204.8	74244.8	36188.3	bdl	9594.2	60.6	121681.9	1.2	2.6	bdl	223.3	43.7	4412.6
2M	20.3	206.7	76635.0	36517.0	bdl	10100.3	56.5	124228.2	1.3	2.6	bdl	265.1	39.6	4857.9
3M	20.3	207.3	73999.8	36320.5	bdl	9938.1	62.8	121597.3	1.4	2.1	bdl	115.7	104.8	4506.8
4M	20.9	208.4	74634.9	38167.7	bdl	10340.6	58.3	125227.0	1.4	2.6	bdl	162.5	104.3	5129.0
1D	20.3	207.5	76447.9	36735.1	bdl	9541.5	39.0	119895.1	1.2	2.0	0.1	1872.1	59.9	5753.0
2D	20.9	207.3	77578.0	37662.2	bdl	10165.9	37.1	124786.1	1.4	2.2	bdl	1489.0	35.3	5720.7
3D	20.9	209.1	77316.6	37743.2	bdl	9908.1	42.0	123580.6	1.3	1.3	bdl	1422.8	109.7	5585.7
4D	20.6	207.7	76759.6	37758.1	bdl	10135.3	49.2	124939.1	1.3	1.7	bdl	677.6	185.1	5471.3
RW	8.0	107.0	42086.5	22092.4	2.6	4254.2	597.4	40235.5	1.1	2.5	0.1	20.6	bdl	5995.2
9PM on 8/16/13														
Well	Li [ppb]	B [ppb]	Na [ppb]	Mg [ppb]	Al [ppb]	Si [ppb]	P [ppb]	Ca [ppb]	Ti [ppb]	V [ppb]	Cr [ppb]	Mn [ppb]	Fe [ppb]	K [ppb]
1S	12.3	126.5	60075.6	31042.0	bdl	15112.4	210.0	152994.9	2.3	2.3	0.2	1882.4	6717.4	1847.0
2S	19.0	197.4	79362.6	35200.4	bdl	9903.9	108.6	134528.1	1.3	0.6	bdl	475.2	395.3	2583.0
3S	18.8	191.3	76412.5	35803.6	bdl	9747.5	70.4	135789.7	1.5	1.4	bdl	321.3	317.0	2718.8
4S	20.7	211.0	79588.1	40906.6	bdl	11449.9	72.8	153387.3	bdl	3.9	0.1	316.9	96.1	3919.4
1M	20.2	207.6	76301.1	36829.5	bdl	10668.0	61.1	128913.3	bdl	2.4	bdl	240.3	31.9	4641.1
2M	20.1	211.4	76197.1	36639.9	bdl	10673.4	60.5	128538.4	bdl	2.2	bdl	265.0	43.3	4903.6
3M	20.7	211.8	75948.5	36926.5	bdl	10815.7	62.9	129709.4	bdl	2.1	bdl	120.1	112.0	4741.4
4M	20.3	210.9	75561.7	38173.4	bdl	10594.3	63.5	127211.6	bdl	2.2	bdl	157.6	93.7	5177.9
1D	20.3	211.4	77794.6	37168.9	bdl	10350.7	35.7	126818.4	bdl	2.3	bdl	1861.9	52.1	5717.3
2D	20.8	212.8	77599.1	37760.9	bdl	10436.7	40.8	126532.1	bdl	1.8	bdl	1517.8	43.9	5707.4
3D	20.2	206.9	76748.6	37079.2	bdl	10440.4	46.9	125523.4	bdl	1.0	0.1	1419.6	128.1	5597.7
4D	20.6	205.1	77931.2	37951.6	bdl	9791.1	46.3	123475.2	1.3	2.0	bdl	589.9	158.0	5444.5
RW	7.7	102.5	40164.9	21865.2	bdl	4157.3	549.0	38845.1	1.4	2.5	bdl	13.2	bdl	5949.9
11PM on 8/16/13														
Well	Li [ppb]	B [ppb]	Na [ppb]	Mg [ppb]	Al [ppb]	Si [ppb]	P [ppb]	Ca [ppb]	Ti [ppb]	V [ppb]	Cr [ppb]	Mn [ppb]	Fe [ppb]	K [ppb]
1S	12.4	124.1	59262.6	31339.0	bdl	15684.5	327.5	154841.9	2.5	2.4	bdl	1948.0	7852.3	1802.8
2S	18.9	193.7	78608.7	34575.9	bdl	6109.1	115.7	132677.2	0.9	0.7	bdl	461.2	485.8	2466.0
3S	19.1	189.2	75494.4	35840.6	bdl	9928.3	68.7	136032.1	1.3	1.3	bdl	317.3	297.3	2759.2
4S	20.5	207.4	79591.6	40762.8	bdl	11103.8	77.2	150897.1	1.6	2.9	bdl	316.8	110.4	3818.1
1M	19.7	202.4	76424.3	36219.4	bdl	9845.4	61.5	123568.6	1.2	2.4	bdl	227.9	43.0	4560.2
2M	20.7	207.3	77311.2	36952.4	bdl	10404.5	53.5	126786.0	1.4	2.3	bdl	257.4	48.0	4889.9
3M	20.2	206.5	75994.4	36185.5	bdl	10167.1	59.6	125306.3	1.4	2.2	bdl	113.9	106.3	4619.6
4M	20.3	206.5	75803.0	37866.6	bdl	9793.4	61.0	123028.9	1.5	2.7	0.1	141.1	91.2	5073.8
4M	20.5	207.1	76218.1	38109.0	bdl	9917.9	59.4	124099.1	1.6	2.3	bdl	132.5	97.4	5197.8
1D	20.3	208.9	79840.7	36995.8	bdl	9975.2	35.1	124566.5	1.2	2.1	bdl	1845.4	41.5	5767.5
2D	20.7	208.1	75938.6	37249.7	bdl	15891.3	43.9	120434.3	1.4	1.7	bdl	1482.2	73.6	5650.9
3D	20.9	207.6	75522.1	37676.7	bdl	9694.5	45.8	120760.0	1.6	1.1	bdl	1418.0	127.7	5469.4
4D	20.8	208.6	76545.4	38060.1	bdl	10068.9	46.7	124723.9	1.2	1.9	bdl	604.9	157.0	5471.6
RW	7.6	100.8	38446.9	21949.8	bdl	4474.4	505.4	39767.8	bdl	2.1	bdl	12.2	4.8	5738.7

Table A11 continued: Cation data by hour

1AM on 8/17/13														
Well	Li [ppb]	B [ppb]	Na [ppb]	Mg [ppb]	Al [ppb]	Si [ppb]	P [ppb]	Ca [ppb]	Ti [ppb]	V [ppb]	Cr [ppb]	Mn [ppb]	Fe [ppb]	K [ppb]
1S	13.7	140.6	63148.8	31949.4	bdl	15589.7	147.2	158296.9	bdl	1.3	0.2	1747.0	4033.9	2091.0
2S	19.3	203.3	90454.0	35583.4	bdl	10654.0	121.0	138452.1	bdl	0.8	0.1	472.9	414.1	3163.2
3S	19.2	190.1	74342.9	35888.3	bdl	10614.7	74.0	138300.7	bdl	1.2	0.1	292.4	275.3	2817.9
4S	20.4	208.2	80165.3	40876.2	bdl	11349.5	77.6	154720.6	bdl	3.3	bdl	317.0	105.6	3970.8
1M	19.9	205.8	77329.0	36656.9	bdl	10697.4	67.9	130646.3	bdl	2.7	bdl	217.1	42.9	4621.6
2M	20.6	209.8	75497.9	36723.1	bdl	10754.3	57.3	128753.8	bdl	2.3	bdl	253.1	41.4	4912.3
3M	20.1	204.9	75966.7	36192.8	bdl	9879.1	59.9	124431.6	1.3	2.1	bdl	111.0	101.6	4608.1
4M	20.4	211.0	75319.0	38373.1	bdl	10648.7	67.2	128143.2	bdl	2.4	bdl	135.6	84.2	5217.5
1D	20.4	211.1	78051.4	37375.3	bdl	10430.8	38.2	127343.4	bdl	1.9	bdl	1859.8	57.0	5803.8
2D	20.0	206.3	78240.7	37064.5	bdl	9506.6	40.1	121752.1	1.1	1.9	bdl	1459.0	46.2	5619.6
3D	20.3	207.2	78389.1	37271.2	bdl	9793.2	42.8	122676.0	1.3	1.1	bdl	1395.2	132.0	5568.8
4D	20.9	212.0	76001.1	38203.0	bdl	10647.1	50.3	127310.5	bdl	1.8	bdl	631.5	159.6	5567.5
RW	7.5	95.3	36835.3	21371.9	bdl	4240.3	450.0	38629.3	1.3	2.3	0.1	19.2	12.5	5469.7
3AM on 8/17/13														
Well	Li [ppb]	B [ppb]	Na [ppb]	Mg [ppb]	Al [ppb]	Si [ppb]	P [ppb]	Ca [ppb]	Ti [ppb]	V [ppb]	Cr [ppb]	Mn [ppb]	Fe [ppb]	K [ppb]
1S	11.4	120.0	55568.9	31372.0	bdl	15171.4	435.5	147359.1	2.6	2.3	0.2	2021.9	9131.5	1672.5
2S	19.3	198.5	80115.9	35544.4	bdl	10175.3	110.9	135803.2	1.4	0.7	bdl	452.6	377.3	2738.8
3S	19.2	190.1	75927.9	35932.9	bdl	10160.3	65.8	136449.0	1.3	1.4	bdl	286.2	271.5	2836.7
4S	20.9	206.0	81289.3	41666.9	bdl	11067.9	72.1	153240.7	1.4	3.1	bdl	303.7	102.0	3862.0
1M	19.8	205.0	78743.0	36485.4	bdl	10023.3	61.3	125680.7	1.5	2.6	bdl	212.4	41.5	4652.8
2M	20.3	206.1	76692.6	36776.6	bdl	10106.9	57.8	124491.3	1.4	2.4	bdl	244.2	37.0	4894.0
3M	20.1	203.9	76131.8	36682.8	bdl	10198.3	58.4	125165.6	1.4	2.1	bdl	110.4	96.6	4622.9
4M	20.6	208.5	74828.4	37997.7	bdl	10462.8	54.4	126299.3	1.4	2.5	bdl	133.9	72.9	5086.3
1D	20.6	208.1	79420.9	37368.8	bdl	9913.0	34.5	124400.0	1.5	1.7	bdl	1826.5	51.4	5750.7
2D	20.8	206.2	77876.7	37474.6	bdl	10154.0	38.3	124980.1	1.4	2.0	0.1	1480.3	36.2	5742.3
3D	21.0	209.5	77846.2	37883.9	3.8	10344.9	43.1	125838.8	1.5	1.3	bdl	1400.1	130.9	5584.3
4D	20.7	208.9	76690.9	37906.5	bdl	10183.8	47.6	124566.6	1.4	1.8	bdl	596.2	143.0	5517.2
RW	7.4	94.8	34834.3	21044.3	bdl	4050.2	429.4	37398.8	1.2	2.1	bdl	20.5	6.3	5119.9
5AM on 8/17/13														
Well	Li [ppb]	B [ppb]	Na [ppb]	Mg [ppb]	Al [ppb]	Si [ppb]	P [ppb]	Ca [ppb]	Ti [ppb]	V [ppb]	Cr [ppb]	Mn [ppb]	Fe [ppb]	K [ppb]
1S	12.7	130.3	60899.0	31240.3	bdl	15615.1	264.6	157552.8	2.5	1.6	bdl	1854.8	6528.3	1778.7
3S	19.1	195.1	75169.2	36351.6	bdl	10453.2	71.3	141073.3	bdl	1.3	bdl	270.1	243.0	2829.5
4S	20.3	210.9	80726.5	41801.2	bdl	11151.7	83.5	158174.9	bdl	2.9	bdl	306.1	94.7	3816.1
1M	19.9	210.2	76930.4	36483.2	bdl	10159.1	60.6	127486.9	1.4	2.7	bdl	225.6	35.8	4597.5
2M	19.3	197.8	79808.4	35829.3	bdl	10169.8	102.0	136897.3	1.5	0.8	bdl	452.3	324.4	2706.0
2M	20.1	211.4	76725.6	36781.2	bdl	10646.9	60.2	128866.8	bdl	2.3	bdl	252.9	37.1	5044.3
3M	20.2	208.1	75937.4	36727.0	bdl	10458.1	64.9	128524.6	bdl	2.4	bdl	109.5	94.1	4689.8
4M	20.2	211.7	74902.1	37943.4	bdl	10383.5	66.1	126411.5	bdl	2.6	bdl	124.6	83.0	5197.7
1D	20.4	210.2	78483.4	37551.4	bdl	10210.8	39.6	128598.1	bdl	1.8	bdl	1857.3	53.5	5798.3
2D	20.9	212.7	76899.0	37531.0	bdl	10488.9	39.6	127407.8	bdl	2.1	bdl	1490.4	40.1	5728.4
2D	25.7	264.8	77410.2	47084.3	bdl	10357.2	73.0	126631.5	bdl	2.3	bdl	1844.8	30.6	5677.6
3D	20.1	207.1	76698.8	36979.6	bdl	9914.4	43.2	124228.3	1.3	1.2	bdl	1392.7	123.3	5673.5
4D	20.8	209.1	75190.1	37396.6	bdl	9981.7	42.3	124027.0	1.4	2.5	bdl	598.2	77.8	5540.5
RW	7.3	96.1	35575.0	20694.9	bdl	4093.3	447.1	39004.2	1.1	2.1	bdl	30.5	bdl	5455.0
FB	bdl	bdl	bdl	bdl	bdl	bdl	bdl	bdl	bdl	bdl	bdl	bdl	bdl	bdl

Table A11 continued: Cation data by hour

7AM on 8/17/13														
Well	Li [ppb]	B [ppb]	Na [ppb]	Mg [ppb]	Al [ppb]	Si [ppb]	P [ppb]	Ca [ppb]	Ti [ppb]	V [ppb]	Cr [ppb]	Mn [ppb]	Fe [ppb]	K [ppb]
1S	13.1	131.2	59864.8	31880.7	bdl	15048.4	281.3	150982.5	2.5	1.6	bdl	1825.7	6582.4	1885.5
2S	20.0	201.9	76731.6	36111.3	1.4	10344.2	115.4	135466.5	1.5	0.7	bdl	464.9	355.8	2730.9
3S	19.6	197.2	73708.4	35770.1	bdl	9849.2	72.9	131938.1	1.7	1.5	bdl	253.8	227.6	2742.8
4S	20.7	209.1	78684.7	41768.5	bdl	10581.6	81.0	150255.1	1.4	3.2	bdl	297.6	109.6	3556.1
1M	21.7	222.6	79564.6	38948.8	2.5	10158.9	75.9	131888.6	1.7	2.9	0.3	237.6	39.1	4594.0
2M	20.1	207.8	74531.3	36527.7	bdl	10111.7	57.5	122157.9	1.4	2.4	0.4	250.1	38.9	4915.2
3M	20.5	206.9	74087.7	36577.0	bdl	10003.5	62.4	122188.2	1.4	2.3	bdl	106.7	89.5	4597.5
4M	20.6	206.7	73455.5	38068.4	2.2	10086.8	60.0	121394.6	1.5	2.7	bdl	120.6	72.6	4927.5
1D	20.7	209.6	77411.5	37374.8	1.5	10381.3	40.4	121756.5	1.6	1.6	bdl	1816.0	55.6	5979.4
2D	20.7	210.5	76326.1	37433.2	bdl	9887.2	43.4	121577.8	1.3	1.9	bdl	1466.7	35.6	5736.0
3D	20.9	209.7	75377.9	37480.9	bdl	9870.7	48.3	120906.0	1.4	1.1	bdl	1383.5	129.0	5526.0
4D	21.2	210.1	75327.6	38187.0	bdl	9941.7	50.1	122617.1	1.5	2.1	bdl	600.5	108.2	5464.5
RW	7.4	98.7	36766.8	20742.3	1.8	4119.9	488.1	37682.7	1.1	2.2	bdl	31.1	8.4	5432.8
9AM on 8/17/13														
Well	Li [ppb]	B [ppb]	Na [ppb]	Mg [ppb]	Al [ppb]	Si [ppb]	P [ppb]	Ca [ppb]	Ti [ppb]	V [ppb]	Cr [ppb]	Mn [ppb]	Fe [ppb]	K [ppb]
1S	12.4	125.2	57373.9	31609.8	bdl	15765.5	366.7	149880.6	2.7	2.0	bdl	1913.1	7957.6	1614.9
2S	19.6	198.8	76569.6	36088.6	bdl	10011.4	115.5	133947.3	1.4	0.5	bdl	451.0	387.1	2600.8
3S	20.0	199.2	74129.7	36065.5	2.0	10172.3	77.8	133145.0	1.6	1.4	bdl	247.3	217.4	2875.7
4S	21.2	209.0	80791.9	42803.0	bdl	10959.7	75.6	154481.3	1.5	3.4	bdl	275.1	75.6	3761.4
1M	20.3	204.7	74320.1	36409.0	bdl	9925.9	63.9	121860.6	1.3	2.6	bdl	225.6	30.4	4371.1
2M	22.0	220.6	79122.4	38854.1	2.0	10214.4	69.6	131314.1	1.8	2.6	bdl	271.0	35.6	4823.4
3M	20.1	203.8	73070.2	36025.5	bdl	10042.8	63.7	120810.6	1.2	2.4	bdl	103.5	82.3	4561.3
4M	20.9	208.5	73671.8	38200.5	bdl	10109.3	61.8	122868.4	1.4	2.6	bdl	115.5	94.4	5047.8
1D	20.8	211.9	78385.3	37347.4	1.9	9929.8	37.8	122621.5	1.4	1.8	bdl	1818.7	40.0	5641.0
2D	20.9	209.2	76160.8	37383.0	1.2	9902.2	41.0	121972.0	1.4	2.1	0.4	1468.0	34.6	5546.6
3D	20.9	209.3	75702.9	37802.3	0.2	9898.3	43.0	122006.3	1.4	1.2	bdl	1390.3	117.6	5517.8
4D	20.9	209.7	74599.4	37798.5	26.7	9734.6	49.8	121879.6	2.2	2.2	bdl	604.5	135.9	5433.2
RW	7.5	99.7	38291.9	20868.1	2.7	4133.1	528.4	37822.8	1.1	2.3	0.4	39.4	10.8	5620.6
Well MW7														
Date and Time	Li [ppb]	B [ppb]	Na [ppb]	Mg [ppb]	Al [ppb]	Si [ppb]	P [ppb]	Ca [ppb]	Ti [ppb]	V [ppb]	Cr [ppb]	Mn [ppb]	Fe [ppb]	K [ppb]
925-2P-MW7	17.9	185.2	66903.4	36209.3	bdl	10211.4	31.9	131188.9	1.5	2.5	bdl	174.2	64.8	3569.0
925-2P-MW7	18.7	193.3	65708.1	36787.3	bdl	10901.4	30.3	135469.2	bdl	2.5	bdl	196.5	95.9	3729.7
816-11A-MW7	19.6	204.0	72975.1	38395.6	1.9	10496.5	31.3	135865.8	1.6	1.2	0.4	531.2	309.4	4123.1

References

Aeschbach-Hertig, W. (2012). Physics of aquatic systems. Part II: Isotope Hydrology. Institute for Environmental Physics. University of Heidelberg.

Basin Highlights Report (2014). A summary of water quality in the Colorado River basin during 2013. http://www.lcra.org/water/Documents/2014-Basin-Highlights-Report.pdf

Boano, F., Demaria, A., Revelli, R., and Ridolfi, L. (2010). Biogeochemical zonation due to intrameander hyporheic flow. Water Resources Research, 46(2).

Briggs, M. A., Lautz, L. K., Hare, D. K. (2013). Relating hyporheic fluxes, residence times, and redox-sensitive biogeochemical processes upstream of beaver dams. Freshwater Science, 32(2), 622–641.

Cardenas, M. B., and Markowski, M. S. (2011). Geoelectrical imaging of hyporheic exchange and mixing of river water and groundwater in a large regulated river. Environmental Science & Technology, 45(4), 1407–11.

Colorado River Corridor Plan. (2011). Travis County, Texas. Transportation and Natural Resources, City of Austin & LRCA. http://www.co.travis.tx.us/tnr/crcp/files/CRCP_Ex_Summ_draft.pdf

Colorado River Watch Network. (2014). Lower Colorado River Authority. https://crwn.lcra.org/

Coplen, T. B., and Kendall, C. (2000). Stable Hydrogen and Oxygen Isotope Ratios for Selected Sites of the U.S. Geological Survey's NASQAN and Benchmark Surface-water Networks. Open-File Report 00-160. USGS.

Dubrovsky, N. M., and Hamilton, P. A. (2010). Nutrients in the Nation's Streams and Groundwater: National Findings and Implications. USGS.

Environmental Protection Agency. (2012). Water: Total Maximum Daily Loads (303d). http://water.epa.gov/lawsregs/lawsguidance/cwa/tmdl/overview.cfm

Fischer, H., Kloep, F., Wilzcek, S. and Pusch, M. T. (2005). A river's liver - microbial processes within the hyporheic zone of a large lowland river. Biogeochemistry, 76, 349-371.

Garner, L.E., and Young, K.P. (1976). Environmental Geology of the Austin Area: An Aid to Urban Planning. The University of Texas at Austin, Bureau of Economic Geology, Report of Investigations No.86.

Gerecht, K. E., Cardenas, M. B., Guswa, A. J., Sawyer, A. H., Nowinski, J. D., and Swanson, T. E. (2011). Dynamics of hyporheic flow and heat transport across a bed-to-bank continuum in a large regulated river. Water Resources Research, 47(3).

Gu, C., Hornberger, G. M., Herman, J. S., and Mills, A. L. (2008). Influence of stream-groundwater interactions in the streambed sediments on NO_3^- flux to a low-relief coastal stream. Water Resources Research, 44(11).

Harvey, J. W., Böhlke, J. K., Voytek, M. A., Scott, D., and Tobias, C. R. (2013). Hyporheic zone denitrification: Controls on effective reaction depth and contribution to whole-stream mass balance. Water Resources Research, 49(10), 6298–6316.

Holmes, R. M., Fisher, S. G., and Grimm, N. B. (1994). Parafluvial nitrogen dynamics in a desert stream ecosystem, Society for Freshwater Science, 13(4), 468–478.

Jones, J.G., Jr. and Mulholland, P.J. (2000). Streams and Groundwaters. Academic Press, San Diego.

Kalff, J. (2002). Inorganic Carbon and pH. Limnology, Chapter 14. Benjamin Cummings, San Francisco.

Kendall, C. and McDonnell, J.J. (1998). Isotope Tracers in Catchment Hydrology. Chapter 2. http://wwwrcamnl.wr.usgs.gov/isoig/isopubs/itchinfo.html

Kottek, M., Grieser, J., Beck, C., Rudolf, B., and Rubel, F. (2006). World Map of the Köppen-Geiger climate classification updated. *Meteorology*, 15, 259-263.

Larkin, R. G., Sharp, J. M. (1992). On the relationship between river-basin geomorphology , aquifer hydraulics , and ground-water flow direction in alluvial aquifers, Geological Society of America Bulletin, 1608–1620.

Lower Colorado River Authority (2013). LCRA Water Quality Data. http://waterquality.lcra.org/

McAllister, Don E. (2001). Biodiversity Impacts of Large Dams. International Union for Conservation of Nature, p. 1-68.

McClain, M. E., Boyer, E. W., Dent, C. L., Gergel, S. E., Grimm, N. B., Groffman, P. M., … Pinay, G. (2003). Biogeochemical Hot Spots and Hot Moments at the Interface of Terrestrial and Aquatic Ecosystems. Ecosystems, 6(4), 301–312.

Mitsch, W. J., Day, J., Gilliam, J. W., Groffman, P. M., Hey, D. L., Randall, G. W., and Wang, N. (1999). Reducing Nutrient Loads, Especially Nitrate-Nitrogen, to Surface Water, Ground Water, and the Gulf of Mexico. Report for the Integrated Assessment on Hypoxia in the Gulf of Mexico. NOAA Coastal Ocean Program.

Olde Venterink, H., Hummelink, E., and Van Den Hoorn, M.W. (2003). Denitrification potential of a river floodplain during flooding with nitrate-rich water: grasslands versus reedbeds. Biogeochemistry, 65(2), 233–244.

Pinay, G., Edwards, R. T., and Naiman, R. J. (2009). Nitrate Removal in the Hyporheic Zone of a Salmon River in Alaska, River Research and Applications, 25, 367–375.

Rodda, P.U., Garner, L.E., and Dawe, G.L. (1969). Geologic Map of the Austin West Quadrangle, Travis County, Texas, University of Texas at Austin Bureau of Economic Geology Geologic Quadrangle Map No. 38.

Sawyer, A. H., Cardenas, M. B., Bomar, A., and Mackey, M. (2009). Impact of dam operations on hyporheic exchange in the riparian zone of a regulated river, Hydrological Processes, 23, 2129–2137.

Sjodin, A. L., Lewis, W. M., and Saunders, J. F. (1997). Denitrification as a component of the nitrogen budget for a large plains river, Biogeochemistry, 39, 327–342.

USGS Dissolved Oxygen Table (2014). U.S. Geological Survey. http://water.usgs.gov/software/DOTABLES/

Zarnetske, J. P., Haggerty, R., Wondzell, S. M., and Baker, M. (2011). Dynamics of nitrate production and removal as a function of residence time in the hyporheic zone. Journal of Geophysical Research, 116.